Examining the role of the promoter region of *het-6* in escape from heterokaryon incompatibility in *Neurospora crassa*

by

Abiodun Laoye

A thesis submitted to the Faculty of Graduate and Postdoctoral Affairs in partial fulfillment of the requirements for the degree of

Master of Science

in

Biology

Carleton University
Ottawa, Ontario

Abstract

Heterokaryon incompatibility (HI) is a form of nonself recognition that limits the formation of heterokaryons – cells that contain genetically dissimilar nuclei. HI is controlled by several *het* loci. One of these, *het-6* is a supergene complex that encodes two tightly-linked incompatibility genes, *un-24* and *het-6*, with allelic variants Oak Ridge (OR) and Panama (PA), and only two natural haplotypes – *un-24*^{OR}*het-6*^{OR} or *un-24*^{PA}*het-6*^{PA}. *het-6* encodes a HET domain protein with no known function outside of incompatibility, whereas *un-24* encodes incompatibility function and the large subunit of ribonucleotide reductase. Strains incompatible at the *het-6* locus can 'escape' from HI by mutation in the *het-6* gene (Type I, ~97%), or suppress HI by mutation in a transcription factor called *vib-1* (Type II, ~3%). This study examined the possible role of the *het-6* promoter region in the initiation of escape, by introducing an ectopic *het-6*^{OR} allele into a strain that carried a null endogenous *het-6*^{OR} allele (IB20). Self-incompatible transformants exhibited delayed escape and aberrant post-escape behavior. A *vib-1* mutant allele was introduced into IB20, and the resulting strain was also transformed with the ectopic *het-6*^{OR}. Transformants displayed Type-II like phenotype, but had slower growth rates than a typical Type II strain. Finally, we constructed a plasmid containing the *het-6*^{OR} allele in which the putative VIB-1^{+} binding site was deleted. Transformation of IB20 with this construct generated a transformant with a Type II-like growth phenotype. This study provides insight into the process of escape.

Acknowledgements

First, I would like to thank Dr. Myron Smith, who welcomed me into his lab over four years ago, and has always been a patient teacher and provided invaluable guidance through the completion of this project. I would also like to thank my committee members, Dr. Bruce McKay, Dr. John Vierula, and Dr. Keith Seifert, for being so generous with their time and knowledge, and helping to direct my efforts. Next, I would like to thank everyone at the Smith lab, for their assistance in matters of science and their wonderful company. Finally, I would like to thank my friends and family for their support, and most especially my mother, for her endless love.

Table of Contents

List of Tables

List of Figures

INTRODUCTION

Allorecognition: Can you see me?

Allorecognition is an organism's ability to distinguish between self and nonself. It is a ubiquitous feature of living organisms that is essential in a wide range of inter- and intra-species interactions. This process generally occurs in three phases: the first step is 'detection', which involves the individual unit (cell or organism) detecting the presence of another biological entity in its environment; the second step is 'recognition', where the detected unit is identified as either 'self' or 'nonself'; and the third step is 'discrimination', where the individual unit takes some action based on the identity of the detected unit and the context of the interaction (Grice and Degnan, 2015).

Allorecognition strategies can largely be divided into three categories based on the desired outcome: (i) recognition of self, (ii) recognition of nonself, and (iii) the simultaneous recognition of self and nonself (Boehm, 2006). In each of the above categories, the efficacy of the recognition system is dependent on an appropriate degree of specificity for self/nonself molecular markers that would ensure that allorecognition is only triggered when necessary. Furthermore, the selection of recognition markers is dependent on the unit of selection (i.e., the whole individual vs. a single cell) and the timescale on which the selection operates (i.e., evolutionary vs. individual timescale). Endogenous quality control mechanisms are responsible for monitoring the specificity and selection of allorecognition markers so as to avoid non-specific triggering of allorecognition (Boehm, 2006).

Self recognition is difficult to study and characterize, and may simply reflect an absence

of non-self recognition. Self recognition is a useful strategy for preventing self-fertilization in many organisms (Boehm, 2006; Smith and Lafontaine, 2013). However, nonself recognition and simultaneous self/nonself recognition face unique challenges. Nonself recognition relies on receptors that do not respond to self-generated ligands; quality control of allorecognition in this instance requires non-reactivity with self ligands as well as broad specificity for a wide range of nonself ligands. Examples of nonself recognition systems include the mating type system found in fungi, and immune defence, which relies on the recognition of pathogen-associated molecular patterns that are particularly common structural characteristics of pathogens (Boehm, 2006). Finally, the ability to distinguish between self and nonself provides the most complex challenge for allorecognition systems; this is overcome in one of two ways. The more common approach is to eliminate and/or functionally inactivate self-specific receptors before they can be deployed in defence; this approach requires that new receptors are screened against all self-structures to prevent self-triggered recognition. The second approach involves a post-hoc evaluation of the interacting ligand to determine its origin (i.e., self vs. nonself); in this case, an intermediary 'flag' molecule may be employed such that the presence of a self ligand would inactivate the progression of the recognition signal whereas a nonself-ligand would trigger downstream events that would ultimately result in destruction of the nonself-ligand source. An example of this is found in the human innate immune system, where complement-mediated tagging is used to target pathogens for destruction. The human complement system is comprised of a network of circulating or cell-surface-bound proteins that include substrates, enzymes and modulators of proteolytic cascades. One of these proteins, C3 binds indiscriminately to both host and pathogen cell surfaces and is spontaneously

activated by central cleavage to form the highly reactive C3a and C3b components. The presence of C3b acts as a marker to target a cell for destruction, and also triggers the formation of C3 convertase that cleaves C3 to increase the amount of C3b present on the cell. A set of structurally similar proteins called regulators of complement activation (RCA) prevent the accumulation of C3b on host cells, either by destabilizing C3 convertase or promoting the degradation of C3b to iC3b by proteolytic factor I. However, the hydroxyl-rich pathogen cell surfaces are more conducive to covalent binding of C3b as well as the stability of C3 convertase (Boehm *et al*., 2006; Lambris *et al*., 2008). Systems that simultaneously recognize both self and nonself ligands are commonly found in immune defence (Boehm, 2006).

Allorecognition systems developed early in evolutionary history and are thought to have been critical in the transition from unicellular life to multicellular life. Phylogenetic studies suggest that this transition to multicellularity occurred in about 25 independent eukaryotic lineages (King, 2004; Rokas, 2008). The high prevalence of multicellularity among plants and animals indicates that such a transitional event occurred very early in evolutionary history, whereas the diversity of unicellular and multicellular lineages among fungi indicates that the transition may have arisen and subsequently been lost in several taxa (King, 2004). Regardless of what lineage multicellularity is observed in, the phenomenon is thought to have conferred certain advantages to individual organisms in the face of environmental pressures. For example, multicellularity is associated with reduction of predation due to larger prey size, improved absorption and digestion of nutrients from the environment, reduced interaction with non-cooperative individuals, increased biological complexity, and division of labor of different cellular processes (e.g., mitosis and motility,

which share the same cellular machinery, typically cannot occur simultaneously in a unicellular context) (King, 2004; Rokas, 2008). The presence of an allorecognition system would have been critical during a transition to multicellularity, regardless of the context of the transition. The ability to recognize and differentiate between self and nonself would help prevent interactions with 'cheaters' who may take advantage of the benefits of multicellularity without contributing to the overall fitness of the organism, or alternatively encourage interactions with genetically dissimilar individuals during sexual reproduction as a means to maintain genetic diversity (Grice and Degnan, 2015).

Allorecognition mechanisms are a ubiquitous feature of all living organisms, but the specific function of an allorecognition system is dependent on its biological context. In clonal marine invertebrates like *Haliclona* sp., contact with conspecific individuals may result in tissue fusion. Tissue fusion with self or closely-related individuals (kin) may increase overall colony fitness as a result of an increase in colony size, competitive ability, and/or survival. Conversely, fusion between unrelated genotypes may result in competition for resources, resorption or death of one member of the chimera, and a loss of competitive ability of the colony as a whole. In these organisms, allorecognition maintains the integrity of 'self' of a colony by limiting nonself fusion (McGhee, 2006). Similarly, transplantation of tissues or organs in humans is restricted by allorecognition. In this instance, nonself recognition is associated with a reaction to the donor major histocompatibility complex (MHC) antigens via direct or indirect allorecognition. Direct allorecognition occurs when recipient T lymphocytes recognize nonself MHC molecules on the transplanted tissue, resulting in rapid destruction of donor cells and rejection of the graft. On the other hand, indirect allorecognition occurs when the donor MHC molecules are processed and

incorporated into self-MHC molecules, and presented on the surface of the recipient's antigen-presenting cells (APC). This results in a T cell response that targets the host tissue instead of the donor tissue. Both direct and indirect allorecognition act to limit nonself fusion (Benichou, 1999). In contrast, during sexual reproduction, nonself recognition is essential for sexual compatibility. Genetic recombination during sexual reproduction results in progeny that combine genetic elements from both parents. If the parents are not closely related, they will tend to carry distinct alleles at a greater variety of genetic loci, resulting in progeny that have novel features. Such novel genotypes may increase the fitness of the progeny in a rapidly-changing environment, as well as providing better defence against pathogens in the environment. In this context, allorecognition promotes nonself interactions to maintain genetic diversity and improve the individual's survivability (reviewed in Kurtz, 2003). Some specific, well-characterized nonself recognition systems will be discussed in the following sections.

Many bacteria and archaea possess a type of adaptive immunity termed the CRISPR-Cas system comprising 'Clustered regularly interspaced short palindromic repeats' (CRISPR), and CRISPR-associated proteins (Cas). First, the exogenous genetic material ('Spacer') from a virus or plasmid is taken up by the cell and integrated into the CRISPR locus. This locus is transcribed and the resulting mRNA is cleaved into small interfering RNAs (siRNAs) that are able to guide nucleases that target complementary sequences ('protospacers') for cleavage. The incorporation of the invasive genetic elements into the CRISPR loci provide a kind of genetic record of vaccination events, and may also provide information about environmental changes over time. CRISPR-Cas systems may vary widely in terms of occurrence, genes, sequences, number, and size across different

genomes. For instance, while most organisms typically contain one or two CRISPR loci, up to 19 distinct loci have been identified in *Methanocalcoccus* and 25 putative CRISPR loci occur in *Methanotorris igneus* (Barrangou and Marraffini, 2014; Grissa *et al*, 2007). The ability of the CRISPR-Cas system to distinguish between chromosomal (self) and foreign (nonself) DNA is necessary to prevent an autoimmune response, which would be fatal to the host cell. Experimental evidence suggests that short (2-5 bp) conserved DNA motifs – called proto-spacer adjacent motifs (PAMs) – may be involved in the discrimination between self and nonself sequences. PAMs are CRISPR-type-specific motifs that are present in the protospacer DNA but not the CRISPR locus, and are thought to be important in the acquisition of spacers as well as in the targeting of the endonuclease complex (Mojica *et al*., 2009; Paez-Espino *et al*., 2013; reviewed in Barrangou and Marraffini, 2014).

The social amoeba, *Dictyostelium discoideum*, is able to form multicellular aggregates in response to starvation, comprising 20-30% 'altruistic' cells that die to form the stalk of the structure, and 70-80% viable 'fruiting' cells that form spores. Differentiation into stalk or spore cells is based on physiological biases of the cells that make up a particular aggregate. Leach *et al*. (1973) observed that cells grown on a glucose-rich medium were predisposed to becoming spores, while cells grown on a glucose-poor medium were more likely to become stalk cells. Araki *et al.* (1994) also observed that cells starved in the mid-late G_2 phase were more likely to form spores, while cells starved in the late G_2 phase were more likely to form the stalk. The cells that form these aggregates have been observed to come from different genetic backgrounds; however, a cell's ability to contribute to the formation of the aggregate is dependent on two polymorphic genes, *tgrB1* and *tgrC1*, which are

necessary for self-recognition and development. These genes are hypothesized to prevent the inclusion of 'cheaters' who will be prone to exploiting the established community, for instance, by contributing a disproportionate amount of spore cells during the formation of the aggregate (Hirose *et al*, 2011).

In a host-parasite relationship, the ability of the host to resist predation by pathogenic microbes is called 'Immunity'. Plants and animals share an evolutionarily ancient mechanism for host defence, known as the 'Innate immune system'. The innate immune system uses germ line-encoded receptors that recognize antigens that are conserved in classes of microbes. Jawed vertebrates have since evolved additional components of their immune system that constitute the 'Adaptive immune system'. The adaptive immune system employs randomly generated receptors that recognize specific bacterial antigens, and are able to retain a 'memory' of any antigen interactions in the event of subsequent exposure to a particular pathogen (Janeway and Medzhitov, 2002; Hoebe *et al*., 2004; Iwasaki and Medzhitov, 2010).

In *Drosophila melanogaster*, two genes have been identified that are important for innate immune defence against pathogens. The *Toll* pathway is essential for survival in the event of fungal infections in addition to its role in embryo development, while the *imd* pathway is essential in antibacterial responses. The existence of these two pathways indicates that *D. melanogaster* possesses distinct pathways for dealing with fungal and bacterial pathogens. Furthermore, genetic screens identified two peptidoglycan recognition proteins (PGRPs) that bind directly to bacterial cells. One of these proteins recognizes Gram-negative bacteria and triggers the *imd* pathway, while the other recognizes Gram-positive bacteria and triggers the *Toll* pathway (Brennan and Anderson, 2004).

The innate immune cells in vertebrates include dendritic cells, macrophages, and neutrophils. The innate immune system employs a set of antigen receptors that are encoded in the germ line. The best characterized example of these are the 'Pattern Recognition Particles' (PRRs), which recognize relatively invariant molecular patterns common to microorganisms of a given class. These structures, called 'Pathogen-Associated Molecular Patterns' (PAMPs), are not necessarily unique to pathogenic microbes. PAMPs are ideal targets for the innate immune system because they tend to be highly similar among members of the same bacterial class, are unique products of microbial pathways, and have essential functions in microbial physiology. Consequently, PAMPs do not readily undergo adaptive evolution and are thus not likely to evade recognition. PRRs are largely categorized into secreted, transmembrane and cytosolic classes. Secreted PRRs (like collectins and ficolins) bind to microbial cell surfaces, activate the classical and lectin pathways of the complement system, and target pathogens for phagocytosis by macrophages and neutrophils. The transmembrane PRRs include the Toll-like receptor (TLR) family and C-type lectins. Expression of TLRs is specific to cell types involved in pathogen recognition. Cytosolic PRRs include the retinoic acid-inducible gene (RIG-1)-like receptors (RLRs) and the nucleotide-binding domain and leucine-rich repeat-containing receptors (NLRs). RLRs recognize viral particles and are expressed in most cell types. NLRs represent a large family of intracellular sensors that detect degradation of peptidoglycan, various forms of stress (like ultraviolet irradiation), microbial products, and non-infectious crystal particles (reviewed in Iwasaki and Medzhitov, 2010).

The adaptive immune system is composed of T and B-lymphocytes, and employs antigen receptors that are generated *de novo* in each organism. The receptors are clonally expressed

and produced via recombination-activation-gene (RAG)-protein-mediated somatic recombination, non-template nucleotide addition, gene conversion, and, in the case of B cells, somatic hypermutation. This results in a random and diverse pool of antigens, which provides two advantages for the adaptive immune system. First, the antigens are highly specific, and can thus specifically elicit an immune response. Second, clonal expression and selection endows the immune system with a mechanism for remembering previous infections if they are encountered again. However, the random nature of the adaptive immune receptors presents the potential for improper triggering of an immune response. The adaptive immune system can potentially activate an immune response against self-antigens, resulting in autoimmunity, or against an innocuous nonself antigen, resulting in an allergy. In order to maximize the efficiency of the adaptive immune system while minimizing damage to self, the innate immune system, which is better-suited to make the distinction between self and nonself, typically triggers the first checkpoint that activates the adaptive immune system. Upon activation by PRRs, innate immune cells like dendritic cells couple information about the identity of an antigen and its microbial origin. Thus, the vertebrate immune system combines the highly specific targeting of the adaptive immune system with the nonself-recognition capabilities of the immune system to increase the efficiency of the immune response while limiting the damage to surrounding uninfected tissue (reviewed in Palm and Medzhitov, 2009; Medzhitov, 2007).

In plants, the first line of defence against pathogen invasion is the rigid cell wall that surrounds every cell. Physical defenses can also include wax layers, cuticular layers, antimicrobial enzymes and secondary metabolites. If a pathogen is able to penetrate this layer and access the cell membrane, the next phase of host defence is a type of innate

immunity that is similar to what is observed in animals. Plant PRRs on the cell surface recognize conserved microbial elicitors called microbial-associated molecular patterns (MAMPs). MAMP-triggered immunity (MTI) results in rapid heteromerization of PRRs, which then initiates downstream MTI signaling (reviewed in Dodds and Rathjen, 2010; Muthamilarasan and Prasad, 2013). However, some pathogens are able to evade detection by PRRs, primarily by the injection of effector proteins into the cytoplasm through the Type III secretion system (TTSS). These effector proteins are highly diverse, and can contribute to pathogen virulence in a number of ways. Effectors can act as transcription factors to activate transcription in the host cell, affect histone packing and chromatin configuration, and/or manipulate host transcription machinery to promote the release of nutrients important for pathogen survival. Effector suppression of PTI results in effector-triggered susceptibility (ETS) of the host plant. To combat MTI suppression and ETS, plants have evolved a set of resistance (*R*) genes that recognize specific effectors. Most *R* genes encode nucleotide binding and leucine-rich region (NB-LRR) proteins, which are able to recognize pathogen effectors from diverse kingdoms. Recognition of an effector by an NB-LRR protein results in effector-triggered immunity (ETI), a faster and stronger version of MTI that results in disease resistance, and in some cases, hypersensitive cell death (HR) of the infected cell (reviewed in Jones and Dangl, 2006; Muthamilarasan and Prasad, 2013).

Nonself recognition in filamentous fungi

As in many other organisms, allorecognition in filamentous fungi is important both during sexual reproduction and asexual growth. During the sexual stage, the ability for two conspecific fungal individuals to successfully undergo sexual reproduction is mediated by a genetically-determined sexual compatibility phenotype, called the 'mating type'. The mating type (*mat*) genes regulate this genetic barrier, in addition to encoding transcriptional regulators that control the expression of many genes required for sexual compatibility and reproduction. Fungal sexual reproduction can be divided into homothallism, pseudohomothallism, and heterothallism, based on the genetic specificity of the interacting partners. Homothallic fungi are self-fertile, and so the nuclei that undergo fusion can be genetically similar, making it difficult to identify discreet mating types in such species. In pseudohomothallism, the strains are self-fertile as seen in true homothallism, but the nuclei involved in the fusion event may not be genetically identical. For instance, in *Neurospora tetrasperma*, a single spore may contain nuclei from opposite mating types, resulting in a self-fertile heterokaryon (Kronstad and Staben, 1997). Heterothallism is characterized primarily by self-sterility such that gamete nuclei must carry different mating types. Heterothallic systems may depend on a single-locus, two mating-type scenario as seen in *N. crassa*, or multilocus, many-allele combinations observed in *Schizophyllum commune* (Kronstad and Staben, 1997; Vaillancourt *et al*., 1997). However, most heterothallic ascomycetes depend on the single-locus, two-allele mating system, thus limiting sexual reproduction to individuals carrying opposite mating specificity. In *Saccharomyces cerevisiae*, the *mat* genes occur in either the MATa or MATα allelic forms, whereas in *N. crassa*, they are designated as either *mat a* or *mat A* (Kronstad and Staben, 1997; Kim *et*

al., 2012).

Many of the signaling and regulatory components that control mating in fungi appear to be widely conserved. For example, recognition of mating type is mediated by the secretion of specific hydrophobic peptide pheromones from haploid cells. These pheromones are detected by transmembrane pheromone receptors, so that cells of one mating type only respond to pheromones of the opposite mating type. When an individual of appropriate mating type is encountered, a protein-kinase signal transduction pathway can then be activated via heterotrimeric G proteins that are linked to the pheromone receptors. Following this signal, the mating partners undergo cellular changes that allow them to undergo cellular fusion (plasmogamy), and subsequently nuclear fusion (karyogamy). Such changes include an increased growth response, spatial differentiation, and closer physical interaction of the mating partners mediated by mating type-specific agglutinins. In *S. cerevisiae* and *Schizosaccharomyces pombe*, the mating type loci encode transcriptional regulatory proteins; the combination of these regulatory proteins through fusion of compatible haploid cells can repress the expression of haploid-specific genes and induce the expression of diploid-specific genes, thus allowing the new diploid cell to undergo meiosis and ascosporogenesis. In *N. crassa*, the 'female' of the mating pair responds to the 'male' pheromones by orienting the growth of specialized mating hyphae, or 'trichogynes' towards the 'male' strain (Kronstad and Staben, 1997).

During the vegetative stages of their life cycles, filamentous fungi exist as multicellular, filaments known as hyphae (sing: hypha), which grow by hyphal tip extension and branching. A frequent event during vegetative growth is the fusion of hyphae through a process called 'anastomosis' to produce a network of interconnected hyphae called a

'mycelium'. When a hyphal fusion occurs between conspecific fungal individuals, such that genetically dissimilar nuclei coexist in a common cytoplasm, the resulting cell is called a 'heterokaryon'. Heterokaryon formation may provide certain advantages for the fungal colony, such as mitotic genetic exchange (also known as the 'parasexual cycle'), increased biomass for more efficient absorption of nutrients from the environment, and complementation of defective nutritional competencies or antibiotic resistance (Glass *et al*., 2000; Smith and Lafontaine, 2013).

Successful formation of a heterokaryon requires both partners of the hyphal fusion to be genetically similar at a set of discreet genetic loci designated as *het* (heterokaryon incompatibility) or *vic* (vegetative incompatibility) loci; a difference at any of these *het* or *vic* loci results in vegetative incompatibility. Vegetative incompatibility is common among filamentous fungi and encompasses two types of behaviors: mycelial incompatibility, which is the formation of a demarcation zone, or 'barrage', at the margin where the incompatible strains meet; and heterokaryon incompatibility (HI), which results in slow, abnormal growth or cell death. Although HI is highly correlated with barrage formation in some species like *Podospora anserina*, the two processes do not appear to be interconnected in other species like *N. crassa* (Micali and Smith, 2006). However, vegetative incompatibility phenotypes are similar across different *het* interactions and among different species, indicating that the pathways that mediate the behavior may share common genetic or biochemical features (Glass *et* al., 2000; Paoletti and Clavé, 2007; Smith and Lafontaine, 2013).

Despite its ubiquity, the ultrastructural features of HI have been examined in only a few model species, including *N. crassa, P. anserina* and *Cryphonectria parasitica*. These

ultrastructural features include septal plugging of dying hyphal segments, vacuolization of the cytoplasm, organelle degradation, and shrinkage of the plasma membrane from the cell wall. Other biochemical features may include DNA fragmentation, decreased RNA production, and an increase in proteolytic and other enzymatic activities. Destruction of the incompatible heterokaryon may be completed in as little as 30 minutes in some species (Glass *et al*., 2000; Glass and Kaneko, 2003).

The exact evolutionary origin of HI is uncertain, but it is thought to function as a fungal innate immune system. The primary biological implication of HI may be in preventing the transfer of deleterious genetic elements such as mycoviruses and senescence plasmids. Fungal viruses generally lack an extracellular phase during their transmission cycle, and depend on cytoplasmic transfer following hyphal fusion for their proliferation. Senescence plasmids may also be passed from one strain to another as a result of mitotic genetic exchange and cytoplasmic mixing, which can happen following hyphal fusion. Hence, the septal plug formation and hyphal compartmentation associated with HI restrict the transmission of deleterious genetic elements when an incompatible heterokaryon is formed (Glass *et al*., 2000; Hutchison and Glass, 2012). HI is known to prevent the transfer of viral elements in *C. parasitica* (Cortesi *et al.*, 2001) and *Ophiostoma novo-ulmi* (Paoletti *et al*., 2006), and to prevent the transfer of deleterious plasmids in *P. anserina* (Aanen *et al*., 2010) and *N. crassa* (Debets *et al*., 1994). HI is also thought to prevent 'resource plundering' by genetically different strains, as seen in *N. crassa* (Debets and Griffiths, 1998). By excluding incompatible strains, heterokaryons formed from genetically identical strains may have better access to nutrients and resources derived from maternal tissues.

het genes and heterokaryon incompatibility

The genes involved in eukaryotic nonself recognition are often organized into tightly-linked gene 'complexes'; the totality of nonself recognition complexes in an organism constitutes a nonself recognition 'system'. Most fungal VI complexes are comprised of two tightly-linked genes (Micali and Smith, 2006; Lafontaine and Smith, 2012). The genes that form VI complexes are largely unrelated, but share at least two characteristics. First, alleles of incompatibility genes at a given *het* or *vic* locus tend to exhibit extensive polymorphism. For example, in *N. crassa* the two possible protein products of the incompatibility gene, *het-6*, are only 68% identical, and the alleles of the *het-C* locus contain a highly divergent region that determines allele specificity. The second tendency is that VI complexes contain one incompatibility gene that has a HET domain. The HET domain contains three conserved blocks of 15 to 30 amino acids distributed within a sequence of about 200 amino acids (Figure 1). In *N. crassa*, HET domains have been identified in *het-6*, a known HI gene, *pin-C*, which is closely linked to *het-C*-mediated incompatibility, and in *tol*, which is a mediator of mating type-associated VI (Paoletti and Clavé, 2007). It is thought that these two features together are essential for the proper functioning of the HI complex. The highly polymorphic nature of the VI genes ensures recognition of an incompatible pairing, and the HET domain protein may trigger a programmed cell death pathway. Paoletti and Clavé (2007) demonstrated that overexpression of the HET domain from *het-E* in *P. anserina* was sufficient to trigger programmed cell death (PCD) independent of incompatibility between the HET-C protein and its partners, HET-D and HET-E. Table 1 summarizes the fungal vegetative incompatibility genes that have been characterized so far (Smith and Lafontaine, 2013).

Table 1. Summary of characterized fungal vegetative incompatibility genes (adapted from Smith and Lafontaine, 2013)

Species/ gene[1]	Allelic (A) or non-allelic (N)	Protein features	Reference
***N. crassa* (11 incompatibility loci identified)**			
mat-A1	N	α domain	Glass *et al*. (1990)
mat-a1	N	HMG box	Philley and Staben (1994)
tol	N	HET domain	Shiu and Glass (1999)
het-c	N	Glycine-rich signal+ incomp domain	Saupe *et al*. (1996)
pin-c	N	HET domain	Kaneko *et al*. (2006)
het-6	N	HET domain	Smith *et al*. (2000)
un-24	N,A	RNRL + incomp	Lafontaine and Smith (2012)
***P. anserina* (9 incomp loci identified)**			
het-s	A	Prion protein	Balguerie *et al*. (2003)
het-C	N	Glycolipid transfer protein	Saupe *et al*. (1994)
het-E	N	HET + NACHT + WD40 domains	Saupe *et al*. (1994)
het-D	N	HET + NACHT + WD40 domains	Espagne *et al*. (2002)
het-R	N	HET + NACHT + WD40 domains	Chevanne *et al*. (2009)
het-V	N,A	Uncharacterized	Chevanne *et al*. (2009)
***C. parasitica* (6 incomp loci identified)**			
vic2	N[2]	Patatin-like phospholipase + P-loop NTPase	Choi *et al*. (2012)
vic2a	N[2]	sec9-like	Choi *et al*. (2012)
vic4-1[3]	N[2]	Protein kinase c-like	Choi *et al*. (2012)
vic4-2[3]	N[2]	NACHT + WD40 domains	Choi *et al*. (2012)
vic6	N	HET domain	Choi *et al*. (2012)
pix6	N	DUF1040 domain of unknown function	Choi *et al*. (2012)
vic7	N[2]	HET domain	Choi *et al*. (2012)

[1]Braces at left indicate interacting members of an incompatibility complex.
[2]Inferred as non-allelic based on presence of two incompatibility-like genes at locus and/or only partial loss of vegetative incompatibility activity when one gene at locus is deleted.
[3]Inferred incompatibility gene based on linkage mapping and bioinformatics.

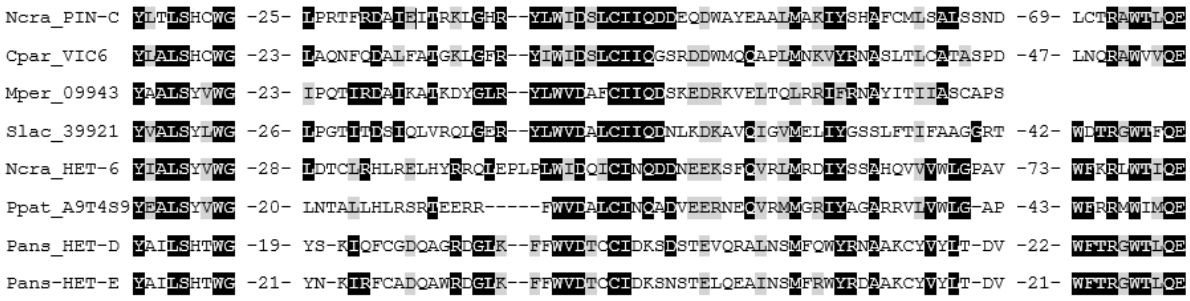

Figure 1. Selected HET-domain sequences from different species. Identical residues at a given position are shaded black, similar residues are shaded grey. Number of amino acids is given for the intervals separating the three conserved blocks of the domain. Abbreviated species names and gene designations are given; Ncra, *N. crassa*; Cpar*, C. parasitica*; Mper, *Monilopthora pernicioasa*; Slac, *Serpula lacrymans*: Ppat, *Physcomitrella patens*; Pans, *P. anserina.* Adapted from Lafontaine and Smith (2013).

The number of *het* or *vic* genes varies among different fungal species. There are at least 11 *het* loci in *N. crassa* (Mylyk, 1975; Bégueret *et al*., 1994), 9 in *P. anserina* (Bégueret *et al*., 1994), 8 in *A. nidulans* (Anwar *et al*., 1993), and 6 in *Cryphonectria parasitica (*Cortesi and Milgroom, 1998). It is interesting to also note that the HET domain does not occur exclusively in genes associated with HI, and there are many more HET domain-encoding genes predicted in fungal genomes than actual *het* loci. In the *N. crassa* genome there are 55 genes predicted to contain HET domain, up to 38 HET domain genes have been found in *Aspergillus* genomes, and *C. parasitica* contains about 96 HET-domain genes (Glass and Dementhon, 2006; Paoletti and Clavé, 2007; Choi *et al*., 2012). The function(s) of these other HET-domain genes remains unknown. Furthermore, some genes that are involved in HI also have additional cellular functions (Table 1; reviewed in Smith and Lafontaine, 2013). For example, in *N. crassa het-c* encodes a signal peptide and *un-24*

encodes the large subunit of ribonucleotide reductase, which is essential for the conversion of ribonucleotides to deoxyribonucleotides. In *P. anserina*, *het-c* encodes a glycolipid transfer protein (Saupe, 2000).

het gene interactions can further be broken down into allelic and non-allelic incompatibility, based on the identity of the interacting partners. Allelic incompatibility involves interactions between different alleles of the same gene, whereas non-allelic incompatibility involves interaction of specific combinations of alleles from two different genes. Take, for example, two HI genes, *A* and *B*, with possible alleles, *A-1* and *A-2*, and *B-1* and *B-2*. An allelic interaction may occur between *A-1* and *A-2* or between *B-1* and *B-2*. On the other hand, a non-allelic interaction may occur between *A-1* and *B-2*, or between *B-1* and *A-2* (Figure 2). Allelic interactions appear to be far less common than non-allelic interactions (Table 1). Only a couple of clear examples of allelic incompatibility have been verified, one involving the *het-s* gene in *P. anserina* (Turcq *et al*., 1990), and the other involving *un-24* in *N. crassa* (Smith *et al*., 2000). Non-allelic interactions appear to be far more common (Smith and Lafontaine, 2013).

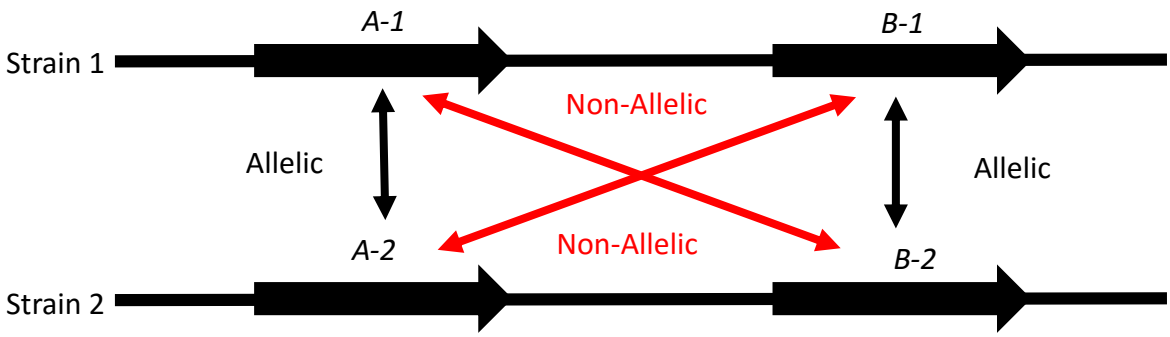

Figure 2. Schematic diagram showing the types of genetic interactions which can mediate HI-associated nonself recognition in filamentous fungi. Allelic interactions are indicated with black double-headed arrows; non-allelic interactions are indicated with red double-headed arrows.

Current understanding of fungal nonself recognition indicates that the process is mediated by protein interactions between incompatibility factors. In *P. anserina* for instance, the *het-s* locus exhibits two polymorphic variants, *het-s* and *het-S*. Co-expression of the HET-s and HET-S proteins triggers an allelic interaction that causes growth inhibition and cell death. However, the HET-s variant can also exist as two alternate phenotypes: [Het-s], which is incompatible with *het-S* strains; and [Het-s*], which exhibits neutral incompatibility. Exposure of a [Het-s*] strain to a [Het-s] strain causes a horizontal transmission of the reactive [Het-s] phenotype to the non-reactive [Het-s*] background. When expressed in the context of incompatibility, the [Het-s] variant behaves much like a prion protein, forming high molecular weight aggregates that accelerate the precipitation of the soluble form of the protein and perpetuate the incompatibility reaction (Dos Reis *et al*., 2002; Horwich and Weissman, 1997). In *N. crassa*, incompatibility at the *het-c* locus is controlled by three allelic variants, *het-c*^{OR}, *het-c*^{PA}, and *het-c*^{GR}. Incompatibility between any of the variants at this locus results in the formation of a stable HET-C heterocomplex that localizes to the plasma membrane of the cell. The presence of the heterocomplex triggers the decline in growth rate and conidiation that is commonly associated with vegetative incompatibility (Sarkar *et al*., 2002). More recently, Reshke (2013) generated a novel *un-24* gene that lacked incompatibility function but retained RNR activity. The study demonstrated that by switching the glutamic acid residue at position 925 in the C-terminal region of the UN-24^{OR} protein, the incompatibility specificity could be manipulated. Switching the glutamic acid to valine (the homologous residue in UN-24^{PA}) conferred PA-like incompatibility, whereas switching the glutamic acid to leucine (the residue found in the large subunit of ribonucleotide reductase (RNRL) of numerous other species) resulted

in a total loss of incompatibility activity. That a single amino acid substitution is able to eliminate the incompatibility activity of UN-24 provides further evidence supporting protein-protein interactions between incompatibility factors as a mechanism for triggering HI.

N. crassa and *P. anserina* have proven to be very useful models for studying HI in filamentous fungi. In *N. crassa*, such analyses have been performed using a few different strategies including the use of heterokaryon tests and partial diploids. Heterokaryon tests make use of two tester strains, each bearing a different auxotrophic marker. When inoculated separately on a minimal medium, these auxotrophic strains are unable to grow; however, when co-inoculated, they are able to complement each other's metabolic deficiency, provided that both strains are also *het* compatible. This test is a relatively simple way to determine the *het* specificity of strains, and was the first method used to establish heterokaryon incompatibility function at the *mat*, *het-c, het-d, het-e* and *het-I* loci (reviewed in Smith *et al*., 1996). The use of partial diploids involves the introduction of an extra copy of a particular sequence into the genome. This can be achieved by carrying out crosses between a translocation-bearing strain and a wildtype strain to produce progeny that bear a duplication of a chromosome segment, or by transforming the DNA of interest into an appropriate strain. When the duplicated sequence encodes an incompatible *het* allele, the resulting partial diploid is said to be 'self-incompatible' (SI), and exhibits a heterokaryon incompatibility phenotype. Partial diploids were used in identifying *het-5, -6, -7, -8, -9,* and *het-10* in *N. crassa* (Mylyk, 1975; Smith *et al*., 1996).

het-6 as a model for HI in *N. crassa*

The *het-6* locus was first identified by Mylyk (1975) as a single locus, but was subsequently shown to be a supergene complex comprised of two tightly-linked genes – *un-24* and *het-6* – with two possible allelic variants at each gene – Oak Ridge (OR) and Panama (PA) (Figure 2). These two genes are under severe linkage disequilibrium such that only two of four possible allelic combinations are found in natural populations; these are the OR haplotype (*un-24*^{OR} *het-6*^{OR}) and PA haplotype (*un-24*^{PA} *het-6*^{PA}) (Mir-Rashed *et al*., 2000; Smith *et al*., 2000). *un-24* encodes the large subunit of a Type I ribonucleotide reductase (RNR), which is the enzyme responsible for reducing ribonucleotides to their

corresponding deoxyribonucleotides. *het-6* encodes a HET-domain protein with no known function aside from nonself recognition (Smith *et al*., 2000; Micali and Smith, 2006; Smith

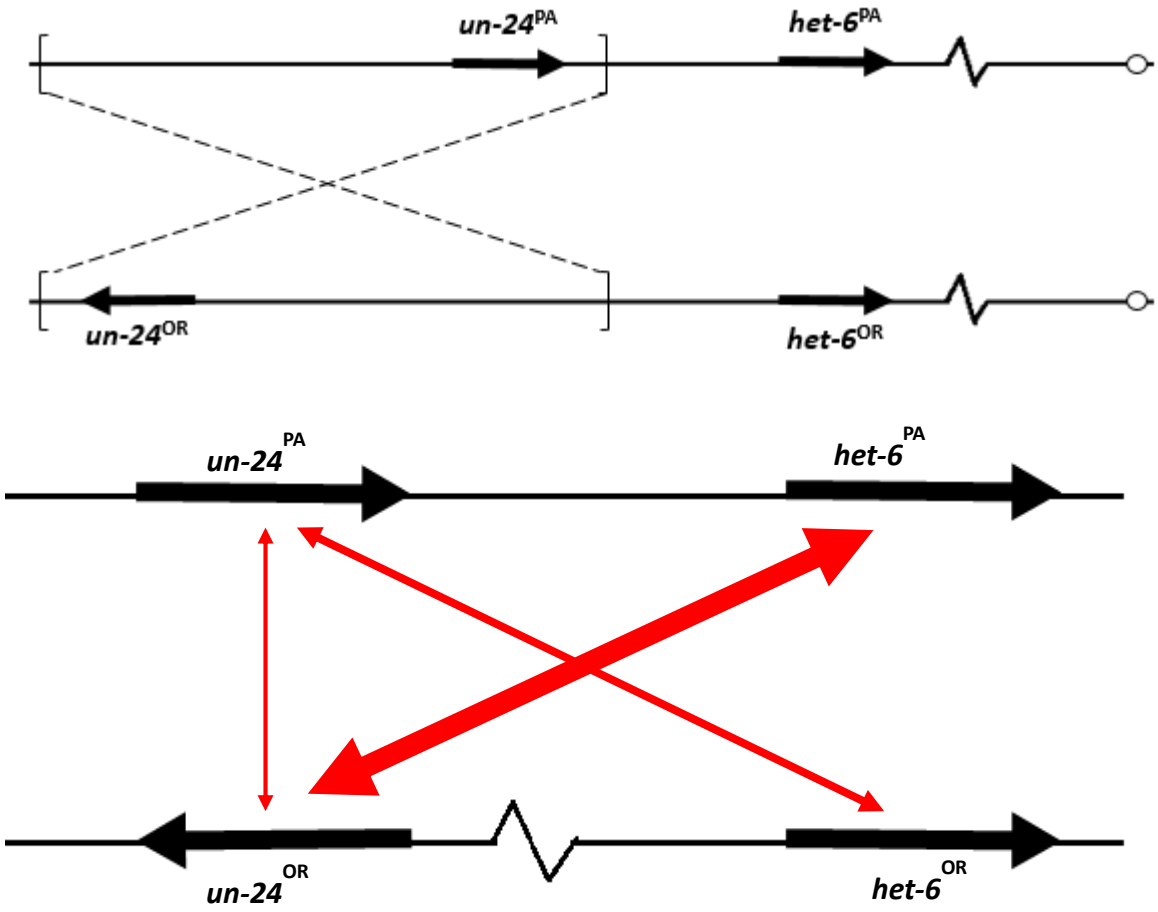

Figure 3. Organization and known interactions of incompatibility genes at the *het-6* locus. (a) Representation of the physical map of Oak Ridge (OR) and Panama (PA) haplotypes of the *un-24-het-6* supergene complex (adapted from Micali and Smith, 2006). The parentheses and dashed lines indicate a paracentric inversion polymorphism which causes the *un-24*^{OR} gene to be in the reverse orientation relative to the *un-24*^{PA} gene. DNA sequence divergence around the inversion breakpoints prevents homologous recombination, resulting to complete linkage disequilibrium of incompatibility genes at the locus. (b) Schematic of the *het-6* locus outlining the known incompatibility reactions (red arrows). The thicker arrow between *un-24*^{PA} and *het-6*^{OR} represents a stronger incompatibility reaction (adapted from Lafontaine and Smith, 2012)

et al., 2013). The incompatibility genes at the *het-6* locus are illustrated in Figure 3.

Type I RNRs are highly conserved, and are found in all eukaryotic species, as well as in some viruses and prokaryotes. They are essential in both *de novo* DNA synthesis and DNA repair. The functional holoenzyme is a tetramer comprised of two large subunits (R1) and two small subunits (R2). Studies in *E. coli* have shown that the reaction mechanism of R1 requires 5 conserved cysteine residues (C225, C439, C462, C754 and C759). In the catalytic site, three cysteine residues (C225, C439 and C462) mediate reduction of the nucleotide through disulfide bond formation. A disulfide exchange involving two cysteine residues located in the C-terminus region (C754 and C759) restores the active site to its reduced form. Glutaredoxin or thioredoxin subsequently reduces the C-terminus disulfide bond to fully regenerate the enzyme. Studies in yeast and with *N. crassa* have shown that the C-terminal cysteine residues of one R1 subunit acts *in trans* to reduce the active site of the neighboring R1 subunit (Smith *et al*., 2013). Allelic incompatibility of *un-24* is proposed to result when an aberrant disulfide bond is formed between cysteines in the *un-24*^{PA} C-terminus (C907 and C918/C921) and the *un-24*^{OR} catalytic site (e.g., C444). Subsequently, an aberrant heterodimeric complex is formed, which may then lead to a toxic higher order protein complex or protein aggregate (Smith *et al.* 2013).

Despite the ubiquity of Type I RNRs, *un-24* is the only described example of an RNR large subunit that also has nonself recognition functions. The *un-24*^{PA} and *un-24*^{OR} alleles share 95% identity, but differ significantly at the 3'end (Micali and Smith, 2006). Using deletion analysis and transformation assays, Smith *et al*. (2000) demonstrated that the specificity region for nonself recognition in *un-24* is encoded by a ~1.6-kbp region located at the 3'-end of the coding sequence.

Whereas differences between the *un-24* alleles are localized to its 3' specificity region, differences between the *het-6* alleles are more evenly spread out over the entire coding region. The DNA sequences of the OR and PA alleles, are 78% identical, while the amino acid sequences share only 68% identity. Micali and Smith (2006) found that, in general, *het-6* has a significantly greater frequency of non-synonymous substitutions between its two alleles, leading to amino acid changes; notable exceptions were found in the regions of the coding sequence that correspond to the conserved HET domain and within an aconitase-like domain. The high levels of nonsynonymous substitutions found in both *het-6* and in the C-terminal region of *un-24* provide evidence that both genes are under diversifying selection (Micali and Smith, 2006), a common feature of nonself recognition genes.

The *het-6* locus is of particular interest in the study of heterokaryon incompatibility for two reasons. First, differences at the *het-6* locus result in one of the most severe heterokaryon incompatibility reactions observed in *N. crassa*. Incompatible heterokaryons and self-incompatible partial diploids exhibit no growth, or at best a much-reduced growth rate (~100 times slower than compatible heterokaryons), are aconidial, and exhibit hyphal compartmentalization and subsequent death (Smith *et al*., 2000). Secondly, *het-6*-mediated HI can result from allelic interactions between opposing alleles of *un-24*, or from non-allelic interactions between *un-24* and *het-6*. The severity of the incompatibility reaction is largely dependent on which of these possible interactions is at play (Figure 2). The weakest reaction is a result of the allelic interaction at *un-24*. Lafontaine and Smith (2012) investigated this interaction by forcing heterokaryon formation between an $un\text{-}24^{OR}$ Δ*het-6* strain and an $un\text{-}24^{PA}$Δ*het-6* strain, and found that a mild form of incompatibility resulted,

which was easily overcome in this context. An intermediate incompatibility is associated with the non-allelic interaction between *un-24*^{PA} and *het-6*^{OR}. Lafontaine and Smith (2012) observed such reactions in synthesized self-incompatible *un-24*^{PA}*het-6*^{OR} strains, in *un-24*^{OR}*het-6*^{OR}: *un-24*^{PA} partial diploids, as well as [*un-24*^{PA}Δ*het-6* + *un-24*^{OR}*het-6*^{OR}] heterokaryons. The allelic interaction at *un-24* was observed to have a minor additive effect in the context of non-allelic incompatibility between *un-24*^{PA} and *het-6*^{OR}. However, the [*un-24*^{PA}Δ*het-6* + *un-24*^{OR}*het-6*^{OR}] heterokaryon exhibited faster growth rate and a different colony morphology when compared to the self-incompatible *un-24*^{PA}*het-6*^{OR}; *un-24*^{PA} homokaryon, indicating that the genetic background of the incompatibility (homokaryotic vs. heterokaryotic) has some effect on the observed phenotype. The interaction between *un-24*^{OR} and *het-6*^{PA} is the most severe incompatibility reaction, resulting in complete growth inhibition and cell death. Heterokaryons formed between *un-24*^{PA}*het-6*^{PA} and *un-24*^{OR} Δ*het-6* strains do not grow, and attempts to transform *un-24*^{OR} into a PA haplotype do not produce any viable transformants (Micali and Smith, 2006; Lafontaine and Smith, 2012).

In the case of the *het-6* locus in *N. crassa*, protein-protein interactions have been observed between the allelic variants of *un-24*. Smith *et al*. (2013) found that self-incompatible *un-24*^{OR}:: *un-24*^{PA} strains expressed a high molecular weight form of the UN-24 protein that consisted of both UN-24^{PA} and UN-24^{OR} subunits. This heterodimer is thought to be rendered stable by the presence of aberrant disulfide bonds between cysteines in the UN-24^{PA} C terminus and the UN-24^{OR} catalytic site, which are resistant to denaturants known to reduce disulfide bonds such as Dithiothreitol (DTT). It is, however, interesting to note that the UN-24 heterodimer can be resolved into soluble UN-24 monomers following

escape from incompatibility (Smith *et al*., 2013).

Overcoming heterokaryon incompatibility

Escape from vegetative incompatibility (or simply, 'escape'), is a process whereby an incompatible colony exhibiting slow growth and an aberrant morphology suddenly converts to a near wild-type phenotype. Escape is characteristic of both incompatible heterokaryons and self-incompatible partial diploids, and typically manifests as a fast-growing sector emanating from the edge, or from within, an incompatible colony. The behavior may originate within a single cell of the SI colony that then rapidly grows out of the SI colony. Escape has been observed for several *het* loci, including *mat, un-24/het-6*, and *het-c/pin-c* incompatibility in *N. crassa*, as well as with *het-R/het-V* and *het-C*/*het-E* incompatibility in *P. anserina*. A variety of processes may mediate escape, including large deletions (Smith *et al.* 1996), chromosomal rearrangements, ectopic recombination and mutation (Chevanne *et al*., 2010). Chevanne *et al*. (2010) demonstrated that escape from *het-R – het-V* self-incompatibility was due to mutations in *het-R,* while escape from *het-C – het-E* self-incompatibility was due to mutations in *het-E.* In both cases, the majority of mutations affected the repeat number or make-up of the corresponding WD-repeat domains of *het-R* or *het-E*, respectively. Lafontaine and Smith (2012) found that escape from *un-24*^{PA} *– het-6*^{OR} incompatibility was associated with point mutations in the *het-6*^{OR} gene, and that following escape, such strains exhibited PA-like specificity. These examples of escape share a peculiar characteristic, which is the ability of the cell to identify and target a particular gene or even allele for mutation in order to initiate the escape. This type of

'directed mutation' is poorly understood and documented, but appears to be at play during escape. Support for directed mutation during escape includes the relative rarity of suppressor mutations associated with escape. Without a mechanism for target preference, one would expect that escape would occur by mutation of a suppressor gene as often as of a VI complex gene. In *N. crassa*, suppressor mutations associated with escape have only been detected in *tol* (for *mat*-associated HI) and *vib-1* (for *het-c/pin-c*- and *un-24/het-6*-associated HI). Escape from *het-6*-associated HI in particular is preceded by mutations in *het-6* in about 97% of cases (Type I escapes), while mutations in *vib-1* are found in only about 3% of cases (Type II escapes). Furthermore, escape timing in some systems, such as in *un-24*^{PA} – *het-6*^{OR} self-incompatibility, appears to be highly regulated, unlike the stochastic behavior that would be expected if escape was mediated by random mutagenesis. In the case of the *het-6* locus, escape from *un-24*^{PA} – *het-6*^{OR} self-incompatibility was observed to occur consistently within 5-8 days of growth at 30°C (Lafontaine and Smith, 2012).

Extragenic suppressors of incompatibility complexes

As mentioned previously, escape from vegetative incompatibility is sometimes mediated by mutations in extragenic elements, which may be upstream or downstream effectors; the presence of a mutation in such 'suppressor' genes may result in partial or total relief from some of the phenotypic aspects of vegetative incompatibility (Xiang and Glass, 2002; Aanen *et al*., 2010). In *P. anserina*, the *mod* (modifier) genes are extragenic suppressors of vegetative incompatibility. Mutations in the *mod-A* gene are associated with escape from

nonallelic incompatibility mediated by the *het-c/het-e*, *het-c/het-d*, and *het-r/het-v* complexes. Mutations in *mod-A* suppress growth inhibition but not hyphal compartmentation and death (HCD); however, a second mutation at the *mod-B* locus may enhance the suppression of HCD, resulting in total suppression of incompatibility. A third *mod* locus, *mod-C*, suppresses *het-R – het-V* incompatibility, but does not have the same effect on other nonallelic interactions (Barreau *et al*., 1998; Xiang and Glass, 2002). In *N. crassa*, vegetative incompatibility associated with the *mat* locus is suppressed in the presence of a recessive mutation at the unlinked *tol* (tolerant) locus. The *tol* gene encodes a 1,011 amino-acid polypeptide that contains a HET domain and a leucine-rich repeat (LRR). LRRs are repeated sequences involved in protein-protein interactions, and are found in proteins that are often associated with recognition functions, such as pathogen recognition gene families in plants (Aanen *et al.,* 2010).

The *vib-1* locus in *N. crassa* has been shown to suppress heterokaryon incompatibility at a number of different loci, including allelic interactions at *mat* and *het-c*, as well as nonallelic interactions at *het-c/pin-c* and *un-24/het-6*. *vib-1* encodes a putative transcription factor containing a conserved DNA binding domain that is also found in Ndt80, a transcriptional activator of genes expressed during meiosis and sporulation in *S. cerevisiae*. Ndt80 is a member of the immunoglobulin-fold family of transcription factors, which includes p53, STAT (Signal Transducer and Activator of Transcription), and NF-κB (Dementhon *et al*., 2006).

Mutations in *vib-1* suppress HI to varying degrees; *het-c/pin-c*- and *mat*-associated HI are abolished, *het-6*-associated HI is only partially suppressed, while incompatibility at *het-e* or *het-8* is suppressed enough to increase recovery of partial diploid progeny but not

enough to alleviate the repression of conidiation and growth (Xiang and Glass, 2004; Dementhon *et al*., 2006). Dementhon *et al*., (2006) demonstrated that *vib-1* is required for the expression of *pin-c*, *tol* and *het-6,* all HI genes encoding HET domain proteins. Thus, mutations in *vib-1* act upstream of *het* genes to suppress the incompatibility phenotype. Furthermore, *pin-c, tol* and *het-6* share a 12-bp consensus sequence, which was identified during a search of the promoter regions of these genes, and is predicted to be a binding site for VIB-1^{+}; this same consensus sequence was found in the set of 55 predicted HET domain genes in the *N. crassa* genome.

While *vib-1* has been shown to be a transcriptional regulator of the *het-6* locus, Lafontaine and Smith (2012) found that mutations in *vib-1* affected the expression of the *het-6*^{OR} significantly, while there was no significant change in the expression of *het-6*^{PA}. Consequently, suppression of HI by *vib-1* is more pronounced in *un-24*^{PA} – *het-6*^{OR} incompatibility than in *un-24*^{OR} – *het-6*^{PA} incompatibility. A proposed explanation for this differential regulation is that it is a result of differences in the number and position of VIB-1^{+} binding sites upstream of the OR and PA alleles. However, it appears that transcriptional regulation of *het-6* is only one of multiple mechanisms employed by *vib-1* in suppressing *het-6*-associated HI. This is supported primarily by the fact that *vib-1* does not negatively regulate the transcription of *het-6*^{PA} and *un-24*, despite suppressing allelic interactions at *un-24* and partially suppressing nonallelic interactions between *un-24*^{OR} and *het-6*^{PA}.

vib-1 belongs to the Ndt80 family of p53-like genes

p53 is a key transcription factor in metazoans that mediates cell response to various stresses, including DNA damage, hypoxia and oxidative stress (Zhang *et al*., 2010). p53 is encoded by a tumor suppressor gene (designated as TP53), and has been implicated in various biological processes, including cell cycle arrest, apoptosis, autophagy, metabolism, and aging (Farnebo *et al*., 2010). A genome-wide gene expression analysis showed that p53 also regulates the expression of genes encoding regulators of transcription, including transcription factors such as E2F7, HES1, HES2 and ZNF219 (Nikulenkov *et al*., 2012).

The p53 protein contains an amino-terminal transactivation domain, a carboxyl-terminal oligomerization domain, and a central DNA-binding domain. The N-terminal transactivation domain is actually comprised of two distinct transcriptional activation domains (TADs), TAD1 and TAD2, which enhance transcription of p53 target genes by recruiting histone-modifying enzymes, components of the basal transcriptional machinery, and coactivator complexes. The C-terminal oligomerization domain facilitates the formation of the active form of p53, which is a tetramer. The extreme C-terminus also contains a basic, lysine-rich domain that contributes to the proper targeting of p53 to its response elements via non-sequence-specific DNA binding, stabilization of p53, and sequence-specific DNA binding. The DNA-binding domain is also important for sequence-specific DNA binding of p53 to its target genes. (Sheikh and Fornace Jr., 2000; Brady and Attardi, 2010).

The activation of p53 in response to various forms of cellular stress is achieved mainly by post-transcriptional modifications (PTMs). p53 undergoes a range of PTMs, which may

include phosphorylation, acetylation, methylation and dimethylation, mono- and poly-ubiquitination, SUMOylation, neddylation, and ADP-ribosylation. The exact combination of PTMs applied to p53 is determined in a stimulus-specific manner, with some PTMs eliciting different responses in p53. Thus, the structural and functional properties of p53 in a particular context is a result of the PTMs that occur in response to that specific stress (reviewed in Gu and Zhu, 2012). The effects of phosphorylation, acetylation and ubiquitination will be discussed in the following sections.

Phosphorylation is one of the major PTMs that affect the function of p53, and can occur at multiple serine residues in the amino- and carboxyl-terminal regions (Zhang *et al*., 1994). p53 can be phosphorylated by cdc2 kinases (Bischoff *et al*., 1990), casein kinase II (Meek *et al*., 1990), casein kinase I-like enzyme (Milne *et al*., 1992) and DNA-dependent protein kinase (Lees-Miller *et al*., 1990), whereas it can be dephosphorylated by protein phosphatase 2A (Scheidtmann *et al*., 1991). The effect of serine phosphorylation is codon-specific. For example, phosphorylation at serine-15 in the N-terminal domain is important for the tumor suppressor function via the inhibition of cell cycle progression (Fiscella *et al*., 1993), while phosphorylation at serine-392 in the C-terminal domain increases the DNA-binding ability of p53 (Hupp *et al*., 1992). In particular, phosphorylation of serine-15 occurs following DNA damage by UV irradiation and ionizing irradiation (Siliciano *et al*., 1997).

p53 may also be activated by acetylation in response to a variety of stresses, including UV irradiation, DNA strand breaks, hypoxia, oxidative stress, and depletion of ribonucleotide pools (Ito *et al*., 2001). The transcriptional coactivators, p300 and CREB-binding protein (CBP), are able to acetylate the C-terminal tail of p53 at lysine-373 and lysine-382 because

of their intrinsic acetyltransferase activity. Acetylation of lysine residues by p300/CBP has been shown to promote increased p53 stability *in vivo*, and is thought to do so by protecting the affected lysine residues from ubiquitination that would target p53 for degradation. Furthermore, acetylation of p53 by p300 increases the DNA-binding activity of p53 (Gu and Roeder, 1997; Ito *et al.*, 2001; Ghosh and Varga, 2007).

While p53 accumulates in the cell in response to stress, in the absence of such stress, wild-type p53 is rapidly degraded. The murine double minute-2 (MDM2) is a RING finger domain containing protein that exhibits E3 ubiquitin-protein ligase activity in its RING finger domain. MDM2 plays a critical role in p53 inhibition, either by binding directly to the N-terminal transactivation domain, or by covalently attaching ubiquitin molecules to p53 via its E3 ligase activity. Direct interaction between p53 and MDM2 results in export to the cytoplasm, while the ubiquitin PTM results in proteasomal degradation. MDM2 is the major E3 ubiquitin-protein ligase that is capable of regulating p53 ubiquitination. The major lysine residues that are ubiquitinated by MDM2 are found in the C-terminal of p53, and include lysine-370, lysine-372, lysine-373, lysine-381, lysine-382 and lysine-386. Since ubiquitination can regulate the degradation of p53, this PTM contributes to the regulation of p53 stability and activity (Oliner *et al*., 1993; Haupt *et al*., 1997; Honda *et al*., 1997; Kubbutat *et al*., 1997; reviewed in Lee and Gu, 2010). Other E3 ligases have been implicated in the ubiquitination of p53, including p53-induced protein with a RING-H2 domain (Pirh2), Trim24, and constitutive photomorphogenesis protein 1 (Cop1), among others (reviewed in Pant and Lozano, 2014).

Interactions between p53 and the genes it regulates is facilitated by the central domain, which mediates sequence-specific DNA binding to p53 response elements located in the

regulatory regions of target genes (Sheikh and Fornace Jr., 2000; Brady and Attardi, 2010). It is a key player in the tumor-suppressive DDR pathways, and is often mutationally inactivated in human cancers (~50% of cases). Most of these mutations are missense mutations in the core domain that incapacitate DNA binding, or confer a gain-of-function that increases the invasiveness and metastasis of tumors (Brady and Attardi, 2010; Reinhardt and Schumacher, 2011). Current knowledge suggests that p53 target genes can be classified into two groups – (i) negative regulators of cell cycle progression, such as p21 cyclin-dependent kinase inhibitor 1A (CDKN1A), and (ii) apoptosis-promoting genes, such as p53 upregulated modulator of apoptosis (PUMA), and genes in the Bcl-2 family (like Bcl-2-associated protein X (BAX) and Bcl-2 antagonist/killer (BAK)). The expression of p53 is under tight regulation, primarily by PTM, as an excess or deficiency of its protein product can be detrimental to the cell. Mutational inactivation of p53 permits uncontrolled proliferation of damaged cells, contributing to the formation of tumors. In contrast, expressions of the dominant active forms of p53 leads to constitutive expression of downstream genes, resulting in degenerative phenotypes and premature aging of the cell. The function of p53 as a regulator of cellular DDR networks is highly conserved in species that possess a TP53 homolog (reviewed in Reinhardt and Schumacher, 2011).

The endpoint of p53 activation is dictated by cell type, environmental context, and the nature of the stress that influence PTM. Under severe or sustained stress, p53 initiates irreversible apoptosis or senescence programs via the transcriptional induction of components of the transmembrane extrinsic and mitochondrial intrinsic cell death pathways. p53 can also induce cellular senescence in response to severe stress. Under lower stress conditions where DNA repair is possible, p53 facilitates temporary cell cycle arrest,

allowing the cell to pause and repair DNA damage (reviewed in Brady and Attardi, 2010). Changes in cellular metabolism and/or nutrient availability can also constitute a form of stress, and p53 has been implicated in the response to these kinds of stress. p53 can limit transport of glucose into cells directly by repressing the expression of glucose transporters, or indirectly through the inhibition of NF-κB. p53 can also repress the insulin receptor promoter to limit glucose transport. This is important in cancer, where tumor cells display elevated rates of metabolism. p53 is able to initiate autophagy in response to genotoxic stress by inducing the activation of the kinase AMPK, which inhibits the mammalian target of rapamycin (mTOR), a master regulator of autophagy. Conversely, p53 inhibits autophagy in unstressed cells (reviewed in Balaburski *et al*., 2010).

Given that p53 is a central hub in stress response in metazoans, it is curious that other eukaryotes, including fungi, do not have a well-defined homolog of p53. However, there are shared features between p53 and Ndt80-like proteins found in fungi. The DNA-binding domain of Ndt80 is a single structural domain comprised of a β-sandwich with two antiparallel β sheets. This domain is identified as a p53-like DNA binding domain and is similar in topology to the N-terminal domain of NF-κB; however, the rest of the DNA-binding domain has no structural similarity to any other known proteins (Montano *et al*., 2002). The β-sandwich is characteristic of an s-type Ig fold, making Ndt80 the first characterized non-metazoan member of the Ig-fold family of transcription factors (Bork *et al*., 1994; Lamoureux *et al*., 2002). The DNA-binding domain selectively binds a DNA consensus sequence called the middle sporulation element (MSE) to activate target gene expression. Approximately 70% of genes activated in the middle phase of sporulation contain the MSE (Lamoureux and Glover, 2006). However, only ~62% of genes induced

by Ndt80 contain an MSE (Chu *et al*., 1998).

Despite the low level of primary sequence conservation between Ndt80 and the metazoan Ig-fold transcription factors, the significant structural and DNA-binding similarities suggest that these proteins might be evolutionarily related. There is evidence that other Ig-fold proteins may also be involved in the regulation of meiosis (Lamoureux *et al*., 2002). For example, the nematode *Caenorhabditis elegans* possesses a p53-like gene, *cep-1*, that is required for chromosome segregation during meiosis as well as for ensuring normal embryogenesis. Like p53, *cep-1* also plays a role in the response to cellular and genotoxic stress (Derry *et al*.,2001). Furthermore, *cep-1* regulation is tightly regulated, as overexpression of CEP-1 is lethal (Derry *et al*.,2001). The Ndt80 and p53 families of proteins may therefore represent analogous protein families, both of which are central regulators of complex cellular pathways. Even though activation of these proteins is in response to different signals (genotoxic stress for p53 vs. meiosis for Ndt80), their expression facilitates the induction of transcription for several downstream targets, ensuring the completion of the appropriate pathway.

Diploid cells of *S. cerevisiae* enter a developmental program of meiosis and sporulation as a response to nitrogen starvation in the presence of a poor carbon source. A transcriptional cascade is initiated when the integration of mating type and nutritional signals leads to the induction of 'early' genes. The early gene products are important for the completion of pre-meiotic DNA replication and the chromosomal events of meiotic prophase. Ndt80 is one of these early genes, and itself induces the expression of >150 genes important for progression into the meiotic nuclear divisions and spore formation (Chu *et al*., 1998; Jin and Neiman, 2016).

There is considerable variation in distribution of Ndt80-like genes among fungal species. Only one basidiomycete species (*Ustilago maydis*) has an NDT80-like gene, in contrast to nine species of ascomycetes (including *N. crassa, C. albicans* and *A. nidulans*), two species of chytridiomycetes (*Batrachochytrium dendrobatidis* and *Spizellomyces punctatus*), and three species of zygomycetes (*Phycomyces blakeleeanus*, *Mucor circinelloides*, and *Rhizopus oryzae*). Furthermore, the number of NDT80-like genes varies from as few as 1 in *S. cerevisiae* and *U. maydis*, to as many as 7 in *R. oryzae* (Katz *et al*., 2013). In general, in species carrying more than one Ndt80-like DNA-binding protein, those involved in sexual reproduction and those involved in other responses to environmental conditions branch separately, with one notable exception being *C. albicans* (Doyle *et al*., 2016)

Members of the Ndt80 family perform diverse functions in different fungal species. However, Ndt80-like proteins share a conserved nutrient-sensing feature, but it is unclear whether this feature is linked to the regulation of other cellular processes like pigmentation and meiosis (Doyle *et al*., 2016). In *A. nidulans*, XprG acts as a regulator of extracellular protease production in response to carbon, nitrogen or sulfur starvation. During carbon starvation, XprG regulates the expression of *brlA*, which is a key regulator of conidiophore development. XprG is thought to be a member of a group of regulatory proteins that act upstream of BrlA, and control both secondary metabolism and asexual/sexual development (Katz *et al*., 2013). The *U. maydis* Ndt80 homolog one (*unh1*) is required for proper teliospore maturation and pigmentation. *unh1* is also important for the completion of meiosis, and the DNA-binding domain is crucial for this function (Doyle *et al*., 2016). *N. crassa* has three NDT80 homologs in its genome, designated as *vib-1*, NCU09915 (*fsd-1*), and NCU04729. *vib-1* mutants suppress HI, display altered conidiation patterns, and are

deficient in protease secretion during nutrient starvation (Dementhon *et al*., 2006; Hutchison and Glass, 2010). Unlike Ndt80, none of these three homologs is required for meiosis but they have been implicated in the production of female reproductive structures (protoperithecia) in *N. crassa* (Hutchison and Glass, 2010). Hutchison and Glass (2010) demonstrated that *vib-1* and *fsd-1* have a synergistic interaction in the initiation of protoperithecial formation. Given that protoperithecial formation is regulated by nitrogen availability, they hypothesize that the nutrient sensing by VIB-1 and FSD-1 is important for the initiation of protoperithecial formation.

Purpose of this study

Allorecognition is ubiquitous among all species, but many of the underlying mechanisms that control allorecognition are not well understood. Filamentous fungi provide a unique context for the study of nonself recognition because of the unusual environment that a heterokaryon provides. The presence of multiple nuclei within a shared cytoplasm generates a unique set of challenges for filamentous fungi that may be reflected in the genes and pathways that are required to initiate and maintain heterokaryon incompatibility when it is triggered. Hence, in addition to providing information on nonself recognition systems in a general sense, the heterokaryon perspective may reveal insights that are specific to a biological system that would be difficult to replicate in other model systems.

Not much is known, for instance, about the specific role of the HET domain in HI. There is some evidence to support the hypothesis that HET domain proteins act as signaling molecules to trigger PCD pathways in the event of HI; reduced expression of HET domain

proteins causes a reduction in *het*-associated PCD, while overexpression of the HET domain from *het-E* is sufficient to induce PCD in *P. anserina* (Paoletti and Clavé, 2007; Smith and Lafontaine, 2013). The specificity of the HET domain to species that exhibit HI suggests that this protein domain may be a key player in HI systems, but what other roles could it play?

The purpose of this study is to examine the role of the promoter region of *het-6* in escape from *un-24 – het-6* self-incompatibility. Using an *un-24*^{PA}-expressing strain of *N. crassa* that has a partial knockout of the endogenous *het-6*^{OR}, we introduced a transgenic *het-6*^{OR} through transformation to observe the effect of the gene translocation on HI as well as on escape. A second construct observed the effect of a *vib-1* mutant allele on the suppression of HI at the ectopic *het-6*^{OR}. Finally, we generated a plasmid construct using PCR-directed mutagenesis to delete the 12-bp putative *vib-1* binding site located upstream of the transgenic *het-6*^{OR}. This construct may be used in future studies examining the role of the VIB-1^{+} protein in suppressing HI.

Material and Methods

Strains and culture conditions

Escherichia coli DH5α chemically competent cells (Invitrogen) were grown on LB media containing chloramphenicol (50 µg/mL in solid agar and 25 µg/mL in broth). All *Neurospora crassa* strains used in this study were cultured on Vogel's minimal medium (VMM) containing 1.5% sucrose, 1.5% agar and supplements as required, unless otherwise indicated (Davis and DeSerres, 1970). *Neurospora crassa* strains used in this study are summarized in Table 2. All strains were grown at 30 °C without shaking, unless otherwise indicated.

Generation of spheroplasts for transformation

Spheroplasts of *N. crassa* were generated using a protocol modified from Royer and Yamashiro (1992). Strains were inoculated on VMM agar slants (~20 slants) for 2 weeks to generate conidia. Conidia were harvested by vortexing slants with ~5 mL liquid VMM, and transferring the resulting solution to a sterile 250 mL beaker. The final solution containing conidia was stored overnight at 4 °C. The following morning, the conidia solution was incubated in a 30 °C shaking incubator at 75 rpm for ~ 4 hours (until about 75% of the conidia exhibited germination tubes). The germinated conidia were transferred to sterile 50 mL centrifuge tubes and centrifuged at 700 rpm for 10 minutes at 4 °C in a refrigerated benchtop centrifuge (Eppendorf, Germany). Conidia were washed twice in 30 mL of 1 M sorbitol, and centrifuged between washes. After the second wash, conidia were

re-suspended in 30 mL of 1 M Sorbitol. 1.2 g of Novozyme were dissolved in 12 mL of 1 M Sorbitol and filter-sterilized; 10 mL of this solution was added to the conidia and incubated at 30 °C with shaking at 75 rpm for 45 minutes – 1 hour; cells were observed under a light microscope to confirm formation of spheroplasts. Spheroplasts were washed twice with ice-cold 1 M Sorbitol (700 rpm, 10 minutes, 4 °C), followed by one wash in Sorb/MOPS/$CaCl_2$ (1M Sorbitol; 10mM MOPS, pH 6.3; 50mM $CaCl_2$). After the final wash, cells were resuspended in Sorb/MOPS/$CaCl_2$ at a concentration of 1-2 x 10^8 spheroplasts/mL. The following were added to the resuspended spheroplasts: (i) 12.5 µL/mL DMSO, (ii) 62.5 µL/mL of 5 mg/mL heparin in Sorb/MOPS/$CaCl_2$, and (iii) 250 µL/mL of PEG/MOPS/$CaCl_2$ (40% PEG/ 10mM MOPS/ 50mM $CaCl_2$). The spheroplasts were mixed gently, and aliquots of 500 µL were transferred to sterile 1.5mL Eppendorf tubes and stored at -80^{O}C.

Transformation of *N. crassa*

Transformation of *N. crassa* was achieved either by electroporation or chemical transformation. *N. crassa* was transformed by electroporation using a protocol modified from Navarro-Sampedro *et al*. (2007). Spheroplasts (~ 8 x 10^7 spheroplasts/mL) were thawed on ice and centrifuged at 3000 rpm for 3 minutes. Spheroplasts were washed twice in 450 µL of 1 M sorbitol, and centrifuged between washes. 100 µL of spheroplasts were transferred to each of five separate 1.5 mL Eppendorf tubes, and ~1 mg of DNA was added to the tubes; spheroplasts were incubated with DNA on ice for 5 minutes. The spheroplast/DNA mixture was transferred to an ice-cold 0.2 cm electroporation cuvette

(Cell Projects, UK), and electroporated using a Bio-Rad Gene pulser (Model: 1652076) with the following parameters: voltage gradient = 1.5 kV; capacitance = 25μF; resistance = 600Ω. After electroporation, 1 mL of 1 M Sorbitol was added to the electroporation cuvette. One mL of the transformation reaction was mixed with top regeneration agar containing 18% Sorbitol, 1X FIGS (Fructose, Inositol, Glucose and Sucrose), and nutritional supplements. The agar mixture was plated on bottom regeneration agar containing supplements, 1X FIGS, and 200 μg/100 mL hygromycin B for the selection of successful transformant colonies. Transformations were incubated at 30 °C for 4-5 days.

The chemical transformation of *N. crassa* was based on a protocol outlined by Royer and Yamashiro (1992). One mg of DNA was incubated with a spheroplast suspension (~ 8 x 10^7 spheroplasts/mL) on ice for 30 minutes. Subsequently, 1 mL of PEG/MOPS/$CaCl_2$ was added to the mixture and incubated for an additional 20 minutes at room temperature. Transformed spheroplasts were mixed with ~6 mL of Vogel's regeneration top agar, and plated on Vogel's regeneration bottom agar containing supplements, 1X FIGS and 225 μg/mL Hygromycin B. Transformations were incubated at 30 °C for 4-5 days.

Introduction of a *het-6*^{OR} transgene

The *N. crassa* IB20 strain was derived from a self-incompatible *un-24*^{PA}*het-6*^{OR} strain that had undergone escape via a rare deletion mutation in the endogenous *het-6*^{OR} gene. Sequence analysis of the DNA from this strain showed that the deletion spanned an 879 bp region, from position -555 to +324 of the *het-6* ORF (Appendix A). Therefore, IB20 is functionally an *un-24*^{PA}Δ*het-6*^{OR} strain.

The pCOR1 plasmid was constructed by inserting the *het-6*^{OR} sequence into the multicloning site (MCS) of pCB1004 (Figure 4; Micali and Smith, 2006). pCOR1 was transformed into IB20 by electroporation, using pCB1004 as a positive control. After the incubation period of 4-5 days at 30 °C, the transformations were scored for the number of colonies on each plate as well as their morphology. Transformant colonies were designated as either 'cloudy' or 'starry' (Figure 6).

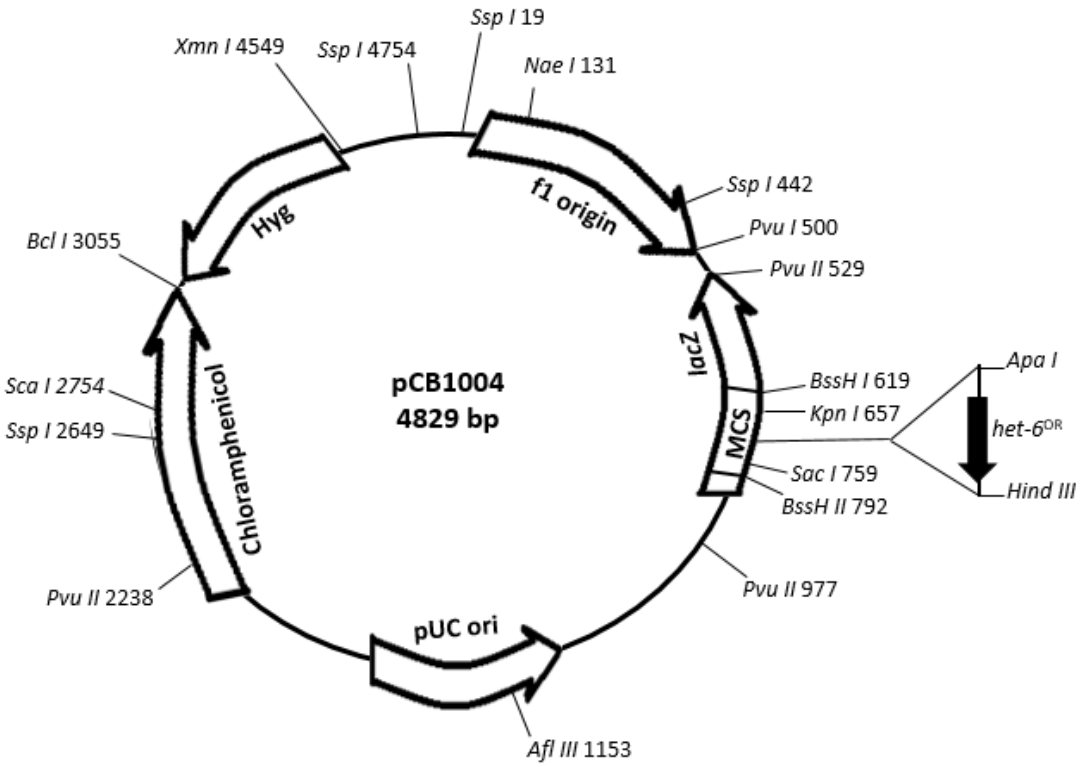

Figure 4. The pCOR1 plasmid is derived from pCB1004, and contains hygromycin and chloramphenicol resistance genes, as well as the ORF of *het-6*^{OR} in the MCS. The pCB1004 plasmid is originally derived from *the pBluescript II* plasmid. Adapted from fgsc.net (2008)

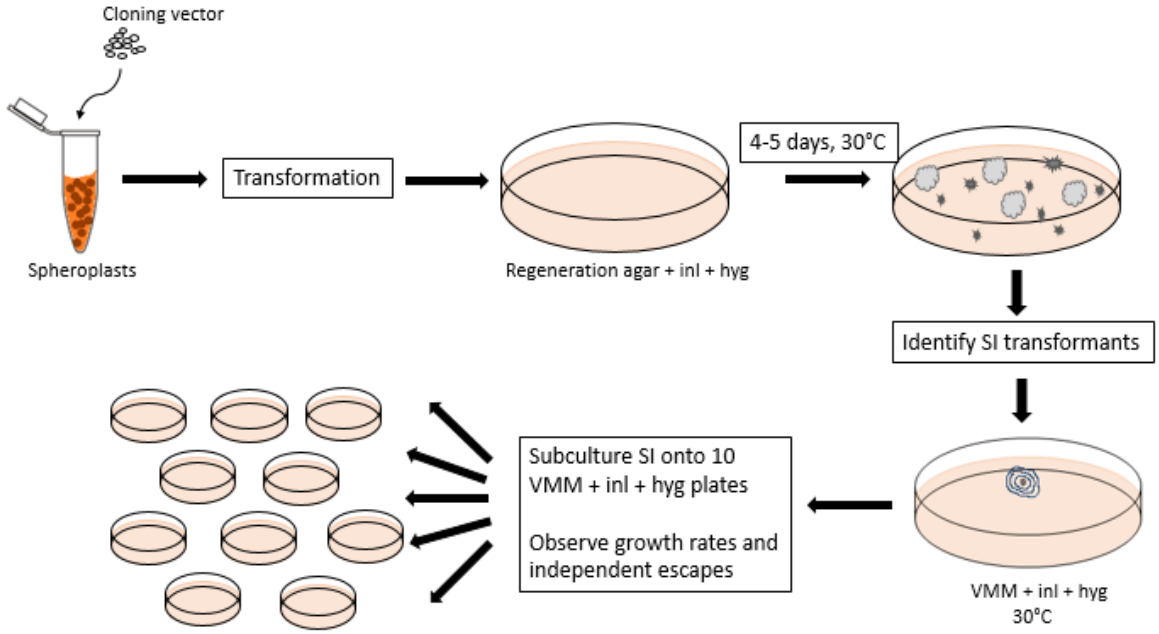

Figure 5. Schematic illustrating the experimental procedure for the introduction of a *het-6*^{OR} transgene in IB20. pCOR1 was transformed into IB20 by electroporation and incubated at 30 °C for 4-5 days. Each transformation plate was scored for number and morphology of transformant colonies. Starry colonies were transferred to VMM agar with inositol and 200 µg/mL hygromycin B to identify SI colonies. Each SI was subcultured onto 10 separate VMM agar plates (inl + hyg) to observe independent escape events.

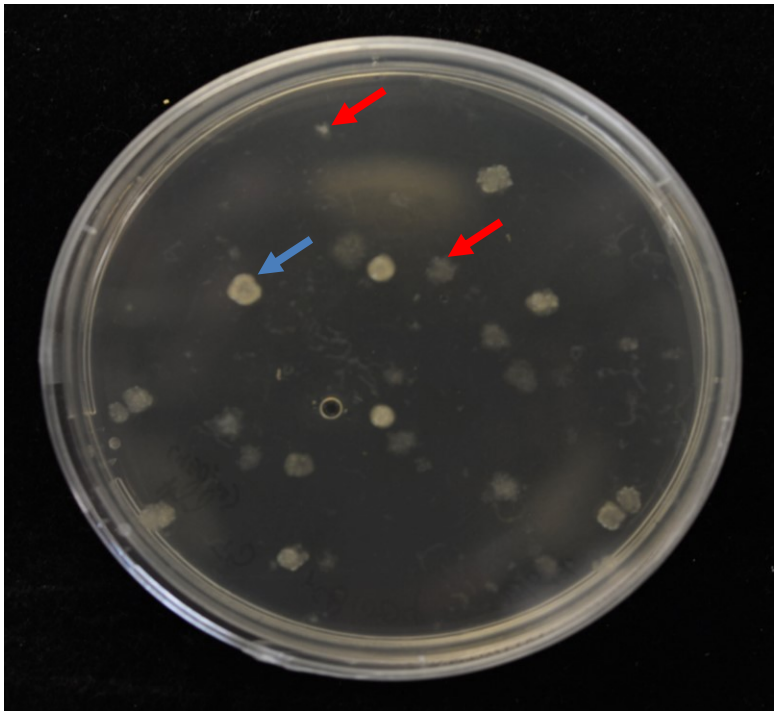

Figure 6. Image of a typical transformation plate showing the colony morphology of cloudy (blue arrow) and starry (red arrows) transformants. Transformants were grown on regeneration agar containing 1X FIGS, 18% sorbitol in the top agar, and 200 µg/100 mL hygromycin B in the bottom agar. Transformations were incubated at 30°C for 4-5 days.

Observation of SI growth rates and escape time

Putative transformants that exhibited a 'starry' morphology on transformation plates were transferred to VMM plates containing 200 µg/mL hygromycin B and observed for 2-3 days of growth. Putative transformants that appeared to have SI-like behavior (slow growth and poor conidiation) were then subcultured onto 10 VMM hygromycin plates to observe independent escape behavior. Growth fronts were marked at ~24 hour intervals until colonies had covered the entire plate. Growth rates were determined in Microsoft Excel. Given a growth front progression of D mm over an interval of T hrs, growth rate (G) was

calculated as:

$$G = \frac{D}{T}$$

The threshold for post-escape growth was chosen as 0.3 mm/hr based on previous work by Smith *et al*. (1996). Since the escape event is frequently observed as a sector of the colony with a more rapid growth rate (> 0.3 mm/hr), the time of escape must be interpolated using post-escape growth rates. Supposing escape was observed at an interval T_e, the time taken for the escape sector to grow (t_e) is determined using the distance grown by the escape sector (D_e) and the first post-escape growth rate after the observation of the escape sector (G_{e+1}):

$$t_e = \frac{D_e}{G_{e+1}}$$

Then, the actual time taken by the colony to escape (E) is determined as the difference between the total time elapsed at observation of escape ($\Sigma(T_1 \ldots T_e$) and the time taken for the escape sector to grow (t_e):

$$E = \Sigma\,(T_1 \ldots T_e) - t_e$$

The escape time for each transformant was taken as the average of the escape time for each individual escape ± standard error. However, it should be noted that this method of determing the escape time only provides an approximation of the actual escape time within ± ~2 hours.

Statistical tests were carried out on the average escape times, pre-escape growth rates, and post-escape growth rates. First, the data sets for each variable were tested for homogeneity

of variance using Levene's test ($\alpha = 0.05$), in order to establish the most appropriate means of comparing the means across groups. If Levene's test indicated that the variance across groups for a particular variable was equal, the means for this variable could then be compared using a one-way ANOVA test ($\alpha = 0.05$) followed by a post-hoc evaluation using the Tukey-Kramer variant of the Honestly Significant Difference (HSD) test (SciStatCalc, 2013). However, if Levene's test indicated that the variance across groups was not equal, the means could be compared using the Kruskal-Wallis test ($\alpha = 0.05$). In this case, post-hoc evaluation was done by pairwise comparison of groups using the Mann-Whitney test (SciStatCalc, 2013).

Suppression of ectopic *het-6*^{OR} by *vib-1*

In *N. crassa, vib-1* has been shown to suppress HI associated with allelic interactions at *mat* and *het-c*, as well as non-allelic interactions at *het-c/pin-c* and *un-24/het-6* (Dementhon *et al*., 2006). To test the ability of a mutant *vib-1* allele to suppress HI at the ectopic *het-6*^{OR}, the strain IB20-V was obtained by crossing IB20 with T2k(0) (Table 2), in order to introduce a *vib-1* deletion mutation in the *het-6*^{OR}(null) background. The cross was carried out as follows:

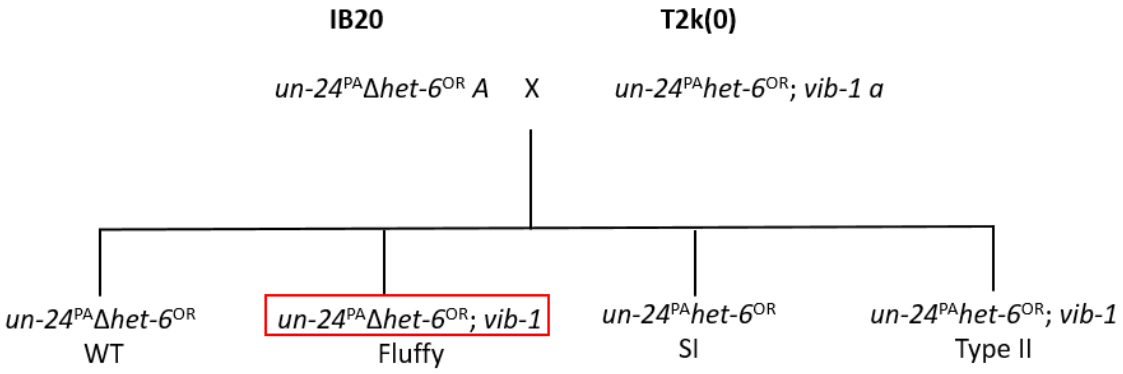

Progeny that carried both the partial knockout and the *vib-1* mutant allele were selected based on a colony morphology of wt-like growth and fluffy conidiation. Spheroplasts of IB20-V were generated and transformed with pCOR1. 'Starry' transformants were selected from the transformation plates and transferred to VMM + inl + hyg plates, and grown at 30 °C. Transformants that behaved like SIs or Type II colonies were subcultured onto 10 VMM + inl + hyg plates to observe growth phenotype. Statistical analyses were conducted on growth rates as outlined above.

Deletion of putative *vib-1* binding site

The putative *vib-1* binding site located ~230 bp upstream of the *het-6* sequence was deleted using a PCR construct on the pCOR1 plasmid (Figure 7a); full details of primers used in this assay are presented in Table 3. Primers were designed that hybridized to the sequences directly adjacent to the *vib-1* binding site; the 3' ends of the primers also contained restriction sites that are recognized by the restriction enzyme *Bsi*WI. PCR was carried out using a high fidelity Phusion DNA polymerase (New England BioLabs; Ipswich, Massachusetts) in a Biometra T-gradient thermocycler (Biometra, Germany). Initial

denaturation was for 5 minutes at 95 °C, followed by 30 cycles of a 1 minute denaturation at 95 °C, 30 second annealing at 60 °C and an extension at 72 °C for 1 minute per kilobase of template. The final extension was for 10 minutes at 72 °C. PCR products were confirmed on a 1% agarose gel using electrophoresis, and the PCR reactions were purified using a FroggaBio Gel/PCR purification kit (FroggaBio, Toronto, Canada). The purified PCR products were subjected to restriction digestion by *Bsi*WI for 1 hour at 55 °C, followed by heat inactivation for 20 minutes at 65 °C. The restriction digest reactions were separated on a 1% agarose gel, and the corresponding product band was purified using the FroggaBio Gel/PCR purification kit (FroggaBio, Toronto, Canada). The purified digested products were then ligated using a DNA Ligase enzyme (New England BioLabs, Ipswich, Massachusetts), and the ligated product was transformed into DH5α cells and grown on solid LB agar containing chloramphenicol at 37^{O}C overnight. Transformant colonies were transferred to LB broth containing chloramphenicol and incubated overnight with shaking at 37^{O}C. Plasmids were extracted from transformant cells using a Promega Wizard miniprep kit (Fisher Scientific, Nepean, Ontario). Deletion of the putative *vib-1* binding site was confirmed by two methods. First, a set of three diagnostic primers were designed; two of these were forward primers while the third was a reverse primer (Figure 7b). One of the forward primers, pCOR1vd1Afw, hybridized to the sequence upstream of the *vib-1* binding sequence; this primer would hybridize to both the wildtype *het-6*^{OR} (from pCOR1) and the deletion construct in pCOR1vd. The second forward primer, pCOR1vd1Bfw hybridized only to the deletion construct in pCOR1vd. The reverse primer, pCOR1vd1rv, was located ~300 bp downstream of the *vib-1* binding sequence and hybridized to both the wildtype *het-6*^{OR} and the deletion construct. PCR amplification was carried out using the

primer combinations (pCOR1vd1Afw + pCOR1vd1rv) and (pCOR1vd1Bfw + pCOR1vd1rv); the resulting PCR fragments were separated using gel electrophoresis on a 1% agarose gel. The deletion construct was also confirmed by sequencing at Genome Quebec Innovation Centre (Montreal, PQ). pCOR1vd was transformed into IB20 by chemical transformation. Growth rates were observed and analyzed using the protocol outlined above.

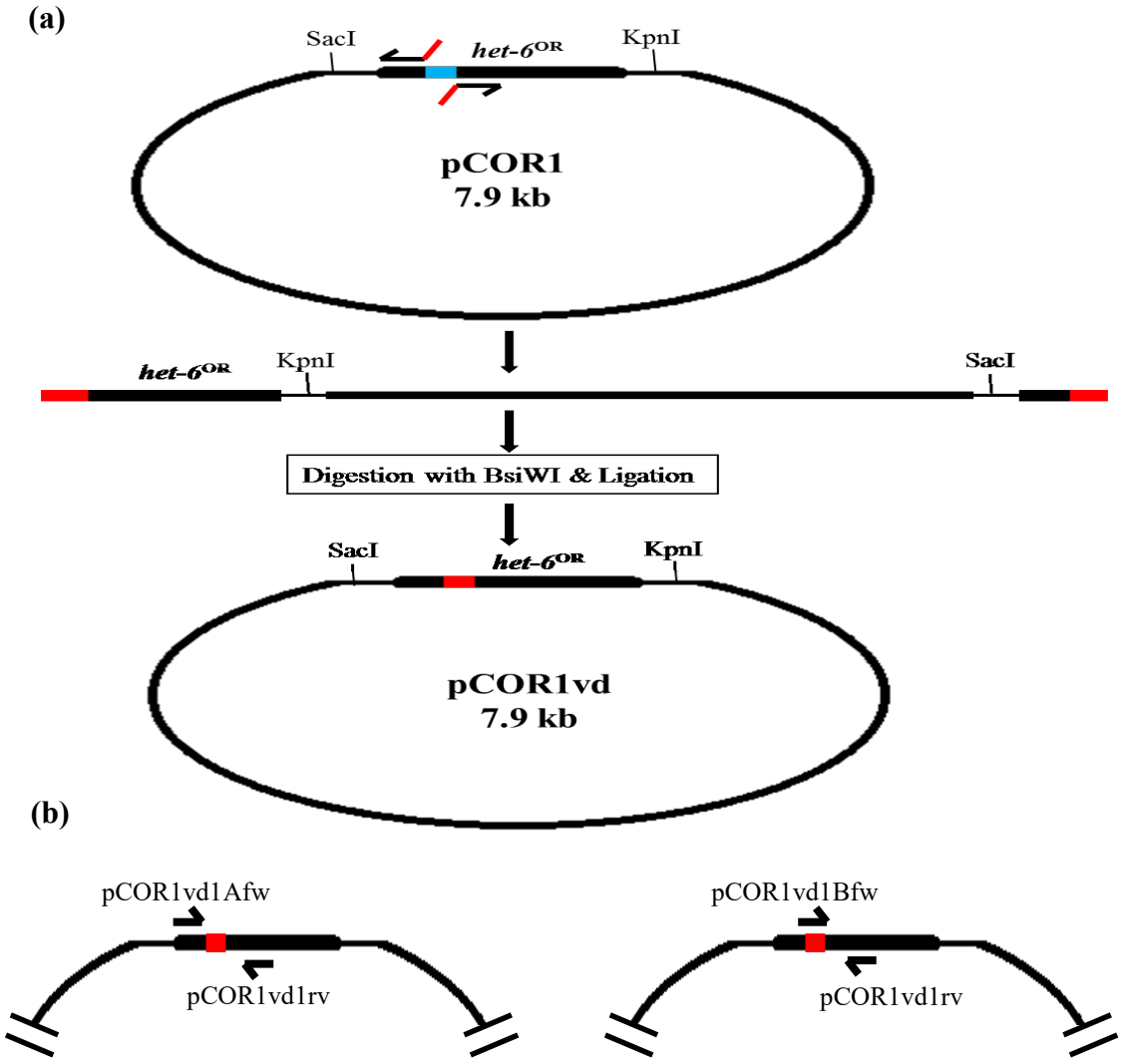

Figure 7. Schematic diagram showing (a) PCR-mediated construct for the deletion of the putative *vib*-1 binding site, and (b) diagnostic PCR to confirm deletion of the putative *vib-1* binding site.

Table 2. Strains used in this study

Strain Name	Genotype	Source
IB20	*un-24*^{PA}Δ*het-6*^{OR}; Δ*mus-52; (inl)*[a] A	I. Buznytska
IB20-V	*un-24*^{PA}Δ*het-6*^{OR}; *vib-1*Δ*mus-52; (inl)*	G. Nourparvar
DLL 8-16	*un-24*^{ts} *Δhet-6::hph; Δmus-52::bar+; inl A*	Lafontaine and Smith (2012)
DLL-T2k(0)	*un-24*^{PA} *het-6*^{OR}*; Δmus-52::bar+; inl vib-1 a*	Lafontaine and Smith (2012)
DLL 14-1	*un-24*^{PA} *het-6*^{OR}; *Δmus-52::bar+; inl* A	D. Lafontaine

[a] Markers in parentheses may be present but were not tested

Table 3. Primers used in this study

Primer Name	Sequence (5' → 3')
	***vib-1* binding site deletion construct**
Het-6ORBsiWIfw[a]	TACGTACGACGCCATTTACCTCGTCATG
Het-6ORBsiWIrv[a]	TACGTACGAAGCAGGGCCCGGTACCAG
	Diagnostic primers for *vib-1* binding site deletion
PCOR1vd1Afw	AATTGGGTACCGGGCCCTGCTTG
PCOR1vd1Bfw	CTGCTTGCCGTACGACGCCATTTTAC
PCOR1vd1rv	GACAGAGCAACCGAGTCATAGCTGAAC

[a] BsiWI restriction site shown as underlined sequence.

Table 4. Cloning vectors used in this study

Vector Name	Size (bp)	Features
pCB1004	4800	Phagemid vector derived from *pBluescript II* with chloramphenicol and hygromycin resistance genes
pCOR1	7221	Phagemid vector derived from pCB1004 with *het-6*^{OR} ORF in multicloning site
pCOR1vd	7215	Phagemid vector derived from pCOR1. Putative *vib-1* binding site is replaced with *Bsi*WI restriction site

Results

Transformation of IB20 with pCOR1 yields SI colonies

The pCOR1 plasmid is a derivative of the pCB1004 vector that carries chloramphenicol and hygromycin resistance genes, as well as a functional *het-6*^{OR} gene inserted between the *Apa*I and *Hin*dIII sites in the MCS of the plasmid. The pCB1004 plasmid, which was itself derived from pBluescript II, was used as a positive control during transformations. Transformations using the pCB1004 plasmid yielded an average of 42 ± 8 colonies/µg DNA, whereas transformations using pCOR1 yielded an average of 14 ± 1 colonies/µg DNA. When broken down by transformant morphology, it was observed that when transformed with pCB1004, 73% of colonies were cloudy while 27% were starry. On the other hand, when transformation was with pCOR1, 61% of the resulting colonies were cloudy, while 39% were starry. pCB1004 and pCOR1 are identical, except for the presence of *het-6*^{OR} in pCOR1.

Escape of incompatible *un-24*^{PA} – ectopic *het-6*^{OR} colonies

Starry transformant colonies from the pCOR1 transformations were transferred to Vogel's minimal medium + inositol (VMM inl) agar containing hygromycin B (hyg) at 2 µg/mL, and incubated at 30 °C. After 2-3 days, 5 colonies that appeared to have the characteristics of self-incompatible colonies (i.e., poor conidiation, slow growth and thin hyphae) were selected and designated as T5.1 – T5.5. Each SI colony was subcultured onto ten individual VMM inl hyg plates in order to observe escape characteristics. For the

purpose of simplicity in this report, I shall refer to the set of 10 subculture plates of a single strain as a 'cohort', while individual plates will be referred to as 'replicates'. Colony growth was observed by marking the edge of the growth front at ~24 hour intervals and growth rate was then determined by taking distance grown at each interval as a function of the time elapsed during the interval. The positive SI control used for these experiments was an *un-24*^{PA}*het-6*^{OR} strain (DLL 14-1) that displayed incompatibility due to the interaction between endogenous *un-24*^{PA} and *het-6*^{OR}. DLL 14-1 does not carry hyg resistance, and was grown on VMM inl plates. SI strains grown on a medium containing hyg tend to grow slower than SIs grown on a medium without hyg. However, the difference in escape time in the presence or absence of hyg is only ~1 day (M.L. Smith, personal communication). Therefore, the use of DLL 14-1 as a control for this construct provides a close approximation of the growth rate and escape time expected in a hyg-resistant SI strain.

The incompatibility reaction between *un-24*^{PA} and ectopic *het-6*^{OR} in the IB20 transformants is illustrated in Figure 8. Escape was observed in 31/31 replicates of the control strain, and in 43/50 replicates across the transformant strains. Table 5 summarizes the frequency of escape in the transformant cohorts observed in this study. A paired Student's t-test was used to determine if there was a difference in the occurrence of escape associated with incompatibility at the endogenous *het-6*^{OR} when compared to the ectopic *het-6*^{OR}. To allow comparison with the five independent cohorts of the ectopic *het-6*^{OR} transformant, the DLL 14-1 cohort was separated so that there were four groups of 6 replicates and one group of 7 replicates (total 31). There was no statistically significant difference in the proportion of replicates that underwent escape ($df = 4$, $p =$

0.099). Escape times for each cohort are summarized in Figure 9. Figure 10 shows sample replicates of the DLL 14-1 strain and an IB20 transformant strain (T5.2), where escape is delayed in the T5.2 replicate as compared to DLL 14-1.

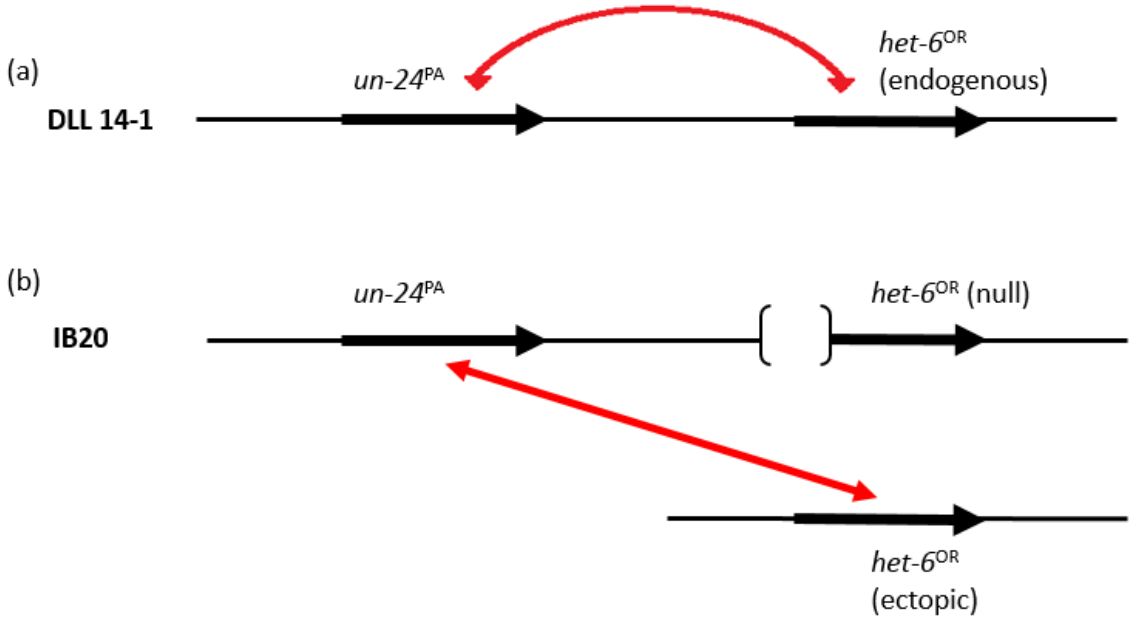

Figure 8. Schematic representing the nonallelic interactions between *un-24*^{PA} and *het-6*^{OR}, as used in this study. Red arrows indicate interactions between the incompatibility genes. (a) In the control strain, DLL 14-1, the endogenous *het-6*^{OR} allele is functional, and confers self-incompatibility in the presence of *un-24*^{PA}. (b) In IB20, the endogenous *het-6*^{OR} allele contains a large deletion spanning -555 to +324 of the ORF, resulting in a null allele. Transformation with pCOR1 introduces an ectopic *het-6*^{OR} allele which interacts with the *un-24*^{PA} allele to induce self-incompatibility.

Table 5. Frequency of escape from self-incompatibility at *het-6*^{OR}

Cohort ID	No. of replicates	No. of escapes
DLL 14-1	31	31
T5.1	10	9
T5.2	10	10
T5.3	10	4
T5.4	10	10
T5.5	10	10

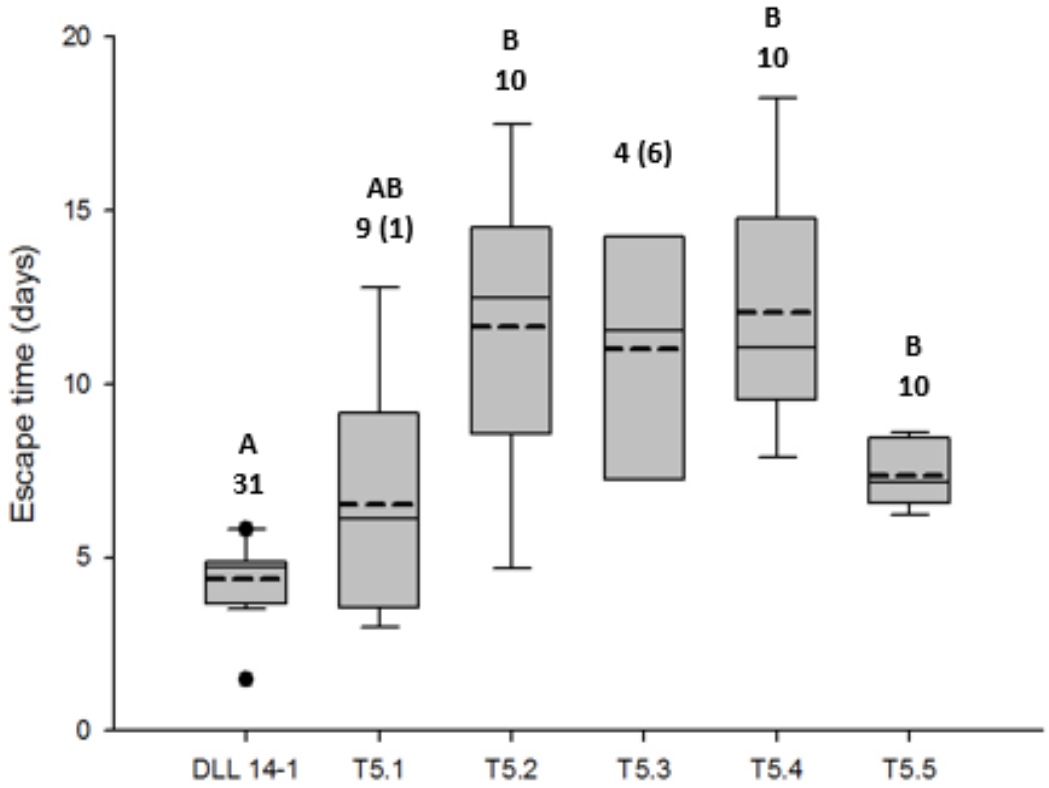

Figure 9. Box plot representing the time taken each cohort to escape from self-incompatibility. The dotted lines in the box plots indicate the mean escape time for each cohort, solid lines inside the box represent the median escape time. Whiskers indicate 5th and 95th percentiles respectively; outliers are represented by solid dots. The same letter above box plots indicate cohorts with statistically similar means. Comparison of means was by Kruskal-Wallis test with post-hoc evaluation using Mann-Whitney test (α= 0.05). Numbers above box plots indicate the number of replicates in each cohort. Numbers in parentheses indicate the number of replicates in which escape was not observed. Such replicates were not included in the statistical analysis. Escape times for T5.3 were not included in the statistical analysis because the sample size was too small ($n < 5$).

(a) (b)

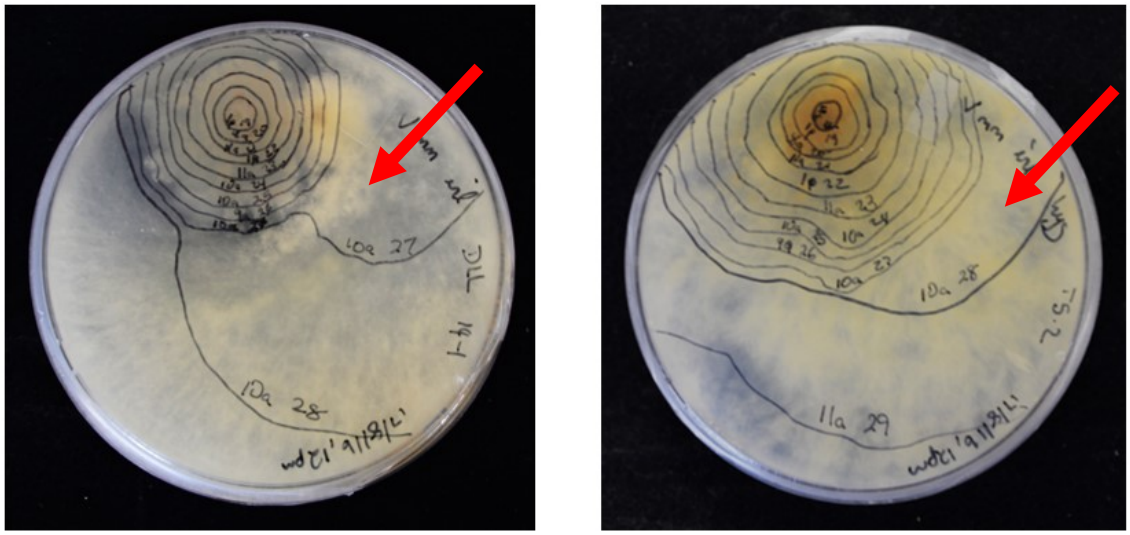

Figure 10. Images showing escape in replicates of (a) DLL 14-1 and (b) T5.2. Red arrows indicate the escape sector. Solid lines indicate time intervals of ~24 hours. DLL 14-1 escaped after 8 days of growth, while T5.2 escaped after 10 days of growth. Strains were grown on Vogel's minimal medium with inositol; T5.2 was grown on medium also containing 200µg/mL hygromycin B. Strains were incubated at 30°C

Levene's test indicated unequal variance across the control and transformant cohorts ($p = 1.87 \times 10^{-3}$, $\alpha = 0.05$). Hence, comparison of means was conducted using the Kruskal-Wallis test, a non-parametric variation of the one-way ANOVA test. There was a statistically significant difference in the mean escape times across cohorts ($H = 41.41$, $p < 0.0001$). The escape times for T5.3 were not included in the Kruskal-Wallis test because of the small sample size. Post-hoc analysis was conducted using the Mann-Whitney test to make pairwise comparisons of cohorts. The mean escape times of the DLL 14-1 cohort ($n = 31$) and T5.1 ($n = 9$) were 4.3 ± 0.14 days and 6.5 ± 1.15 days, respectively. There was no statistically significant difference between these cohorts ($z = -1.41$, $p = 0.16$). However, there was a statistically significant difference when comparing the mean escape time of the DLL 14-1 cohort with T5.2 (11.6 ± 1.37 days; $n = 10$; $z = -3.73$, $p < 0.001$),

T5.4 (12.1 ± 1.05 days; n = 10; z = -4.71, $p < 0.001$) and T5.5 (7.4 ± 0.29 days; n = 10; z = -4.23, $p < 0.001$). Overall, escape times tended to be later in strains expressing *het-6* ectopically than the strain expressing *het-6* in the endogenous location.

Comparison of pre-escape and post-escape growth rates

Using previous work from Smith *et al*., (1996), the threshold for post-escape growth was set at G(post) ≥ 0.3 mm/hr. In addition, all growth rates taken after the observation of the escape sector were considered to be post-escape growth rates, regardless of whether they were lower than the post-escape threshold. The pre-escape and post-escape growth rates for the different cohorts are summarized in Figure 11.

Levene's test was conducted on the pre-escape growth rate, and the result indicated that the variance among cohorts was equal ($p = 0.77$, $\alpha = 0.05$). Consequently, a one-way ANOVA was used to compare the mean pre-escape growth rates. There was a statistically significant difference in the mean pre-escape growth rate across the cohorts ($F(5, 582)$, $p < 0.001$). Post-hoc analysis with the Tukey-Kramer Honestly Significant Difference method indicated that there was no statistically significant difference between the mean pre-escape growth rate of the DLL 14-1 cohort ($0.14 \pm 6.8 \times 10^{-3}$ mm/hr) and that of T5.1 (0.14 ± 0.021 mm/hr) and T5.3 (0.14 ± 0.018 mm/hr). There was a statistically significant difference when comparing the mean pre-escape growth rate of the DLL 14-1 cohort with T5.2 (0.12 ± 0.016 mm/hr), T5.4 (0.087 ± 0.015 mm/hr), and T5.5 (0.12 ± 0.01 mm/hr). Overall, pre-escape growth rates tended to be lower in strains expressing *het-6* *e*ctopically than the strain expressing *het-6* in the endogenous location.

When testing for homogeneity of variance in the post-escape growth rates, Levene's test indicated that the variance among cohorts was unequal ($p < 0.001$, $\alpha = 0.05$). Comparison of the mean post-escape growth was done using the Kruskal-Wallis test, which indicated that there was a statistically significant difference in the mean post-escape growth across the cohorts ($H = 46.08$, $p < 0.001$). The Mann-Whitney test was applied to pairwise comparisons of cohort post-escape growth rates. There was no statistically significant difference when comparing the DLL 14-1 cohort (1.21 ± 0.029 mm/hr) with T5.1 (1.12 ± 0.24 mm/hr; $z = 1.55$, $p = 0.11$) and T5.4 (1.08 ± 0.19 mm/hr; $z = 0.91$, $p = 0.36$). There was a statistically significant difference when comparing the DLL 14-1 cohort with T5.2

(0.71 ± 0.14 mm/hr; z = 4.5, p < 0.001), T5.3 (0.47 ± 0.16 mm/hr; z = 4.84, p < 0.001),

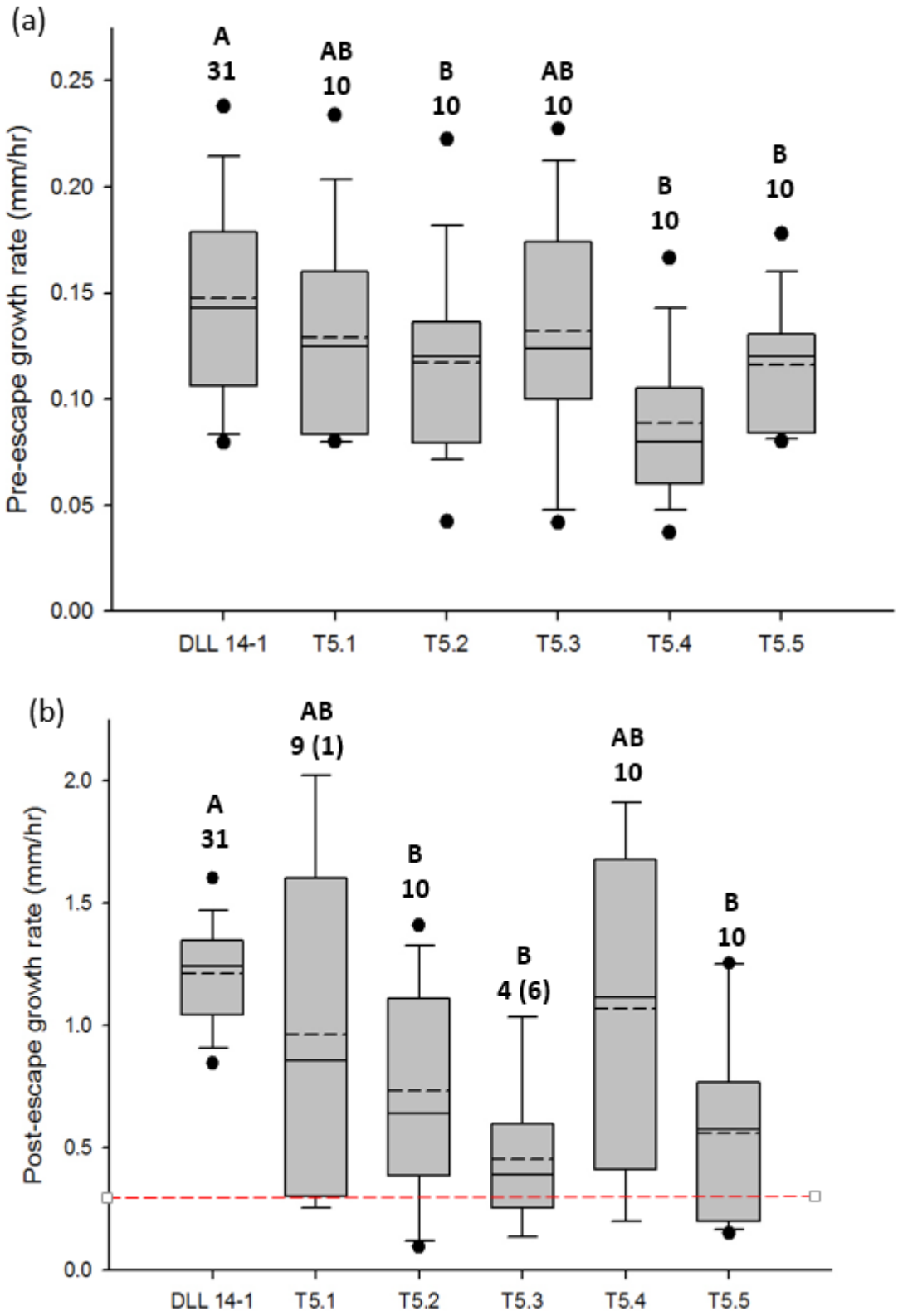

Figure 11. Box plots representing (a) pre-escape growth rates, and (b) post-escape growth rates for self-incompatible strains. The black dotted lines in the box plots indicate the mean growth rate for each cohort, solid lines inside the box represent the median growth rate. Whiskers indicate 5th and 95th percentiles respectively; outliers are represented by solid dots. Letters above box plots indicate cohorts with statistically similar means. Numbers above box plots indicate the number of replicates in each cohort. Numbers in parentheses indicate replicates for which escape was not observed. In (a), comparison of means was by one-way ANOVA followed by post-hoc analysis using Tukey-Kramer Honestly Significant Difference test ($\alpha = 0.05$). In (b), comparison of means was by Kruskal-Wallis test with post-hoc evaluation using Mann-Whitney test ($\alpha = 0.05$). Red dashed line represents the threshold for post-escape growth rate of 0.3 mm/hr.

and T5.5 (0.56 ± 0.12 mm/hr; $z = 6.11$, $p < 0.001$). Generally, post-escape growth rates tended to be lower in strains expressing *het-6* ectopically in comparison to the strain expressing *het-6* in the endogenous location.

Of interest, the post-escape growth rates of the transformant strains were often more variable in strains expressing *het-6* ectopically compared to the strain expressing *het-6* in the endogenous location. In the DLL 14-1 cohort, once the escape sector emerged, the colony growth rate remained above the 0.3 mm/hr threshold, with a minimum post-escape growth rate of 0.83 mm/hr. In comparison, the transformant strains expressing *het-6* ectopically reverted to sub-threshold post-escape growth rates on some of the replicate plates. For example, 2/9 T5.1 escapes reverted to sub-threshold post-escape growth rates, as did 3/10 for T5.2, 2/4 for T5.3, 1/10 for T5.4, and 4/10 for T5.5 (data not

shown, e.g. shown in Figure 12).

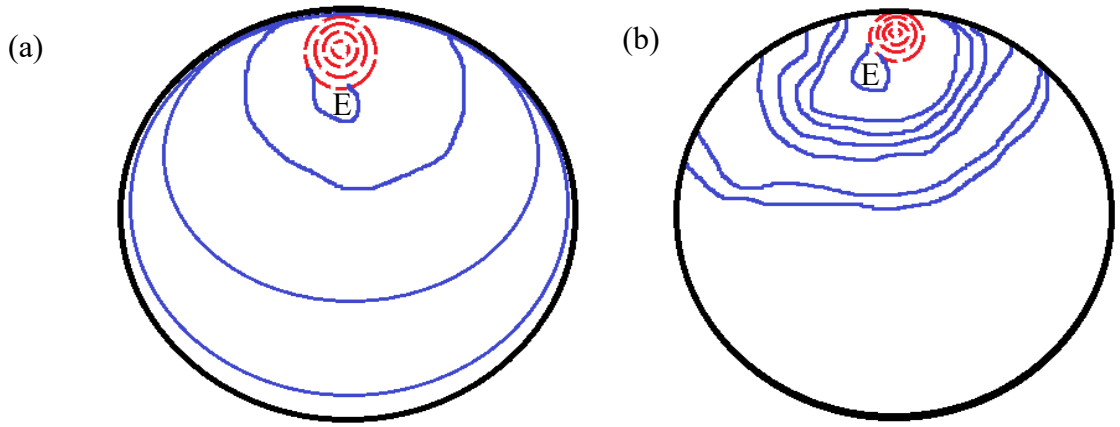

Figure 12. Schematic diagram representing examples of the observed post-escape behavior of (a) DLL 14-1, and (b) ectopic *het-6*^{OR} transformants. Red dashed lines represent pre-escape growth fronts, while blue solid lines represent post-escape growth fronts. The escape sector is denoted as E. In b, after about 2 days after escape, the strain reverts to a pre-escape grow rate.

vib-1 suppression of HI associated with ectopic expression of *het-6*^{OR}

The strain IB20-V was transformed with pCOR1 by electroporation, and transformants were transferred to V mm + inl + hyg. Four transformants that behaved like Type II SIs were identified, and designated as T6.1-T6.4. Each transformant was subcultured to generate cohorts of 10 replicates, and growth rates were observed. The control strain used in this instance was T2k(0), which has a functional endogenous *het-6*^{OR} and underwent Type II escape by spontaneous mutation of *vib-1*. T2k(0) does not carry hyg resistance, and was grown on VMM inl plates. As mentioned previously, strains grown in the presence of hyg tend to grow more slowly than those grown in the absence of hyg.

However, for the purpose of comparison to the IB20-V transformant strains, T2k(0) provides an approximation of the growth rate expected in a hyg-resistant Type II strain.

The growth rates of the control and transformant cohorts are summarized in Figure 13. Levene's test indicated unequal variance among the cohorts ($p < 0.001$; $\alpha = 0.05$), and hence, the Kruskal-Wallis test was applied to compare the mean growth rates. There was a statistically significant difference in the mean growth rates among the cohorts ($df = 4$; $p < 0.001$). Post-hoc analysis with the Mann-Whitney test indicated that there was a statistically significant difference in the mean growth rate when comparing the DLL T2k(0) cohort (0.66 ± 0.014 mm/hr) with T6.1 (0.32 ± 0.023 mm/hr; $p < 0.001$), T6.2 (0.37 ± 0.031 mm/hr; $p < 0.001$), T6.3 (0.22 ± 0.016 mm/hr; $p < 0.001$), and T6.4 (0.18 ± 0.0084 mm/hr; $p < 0.001$). In general, the growth rates of the transformant cohorts were lower than those observed in the control cohort. However, similar to the DLL T2k(0) control, most growth rates in the transformant cohorts were greater than the SI pre-escape growth rates. Figure 14 shows the growth phenotype of sample replicates of T2k(0) and a

transformant of IB20-V (T6.1)

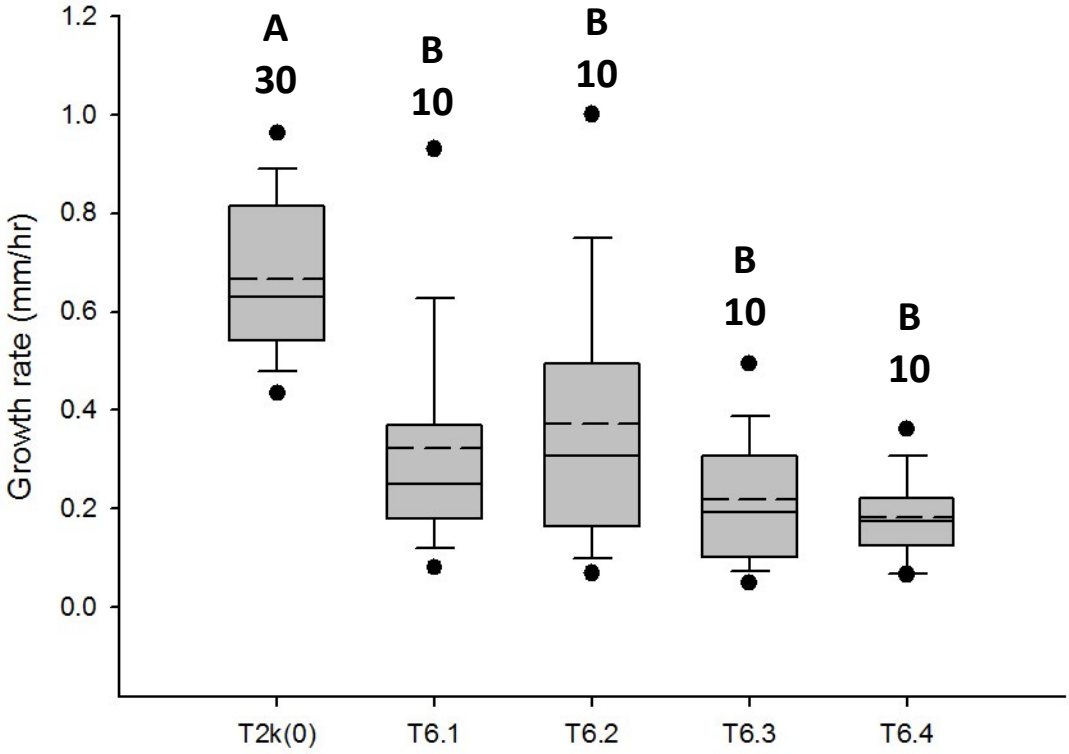

Figure 13. Box plots representing the growth rates of self-incompatible strains which also carry a *vib-1* deletion mutation. The black dotted lines in the box plots indicate the mean growth rate for each cohort, solid lines inside the box represent the median growth rate. Whiskers indicate 5th and 95th percentiles respectively; outliers are represented by solid dots. Letters above box plots indicate cohorts with statistically similar means. Numbers above box plots indicate the number of replicates in each cohort. Comparison of means was by Kruskal-Wallis test with post-hoc evaluation using Mann-Whitney test (α= 0.05).

(a) (b)

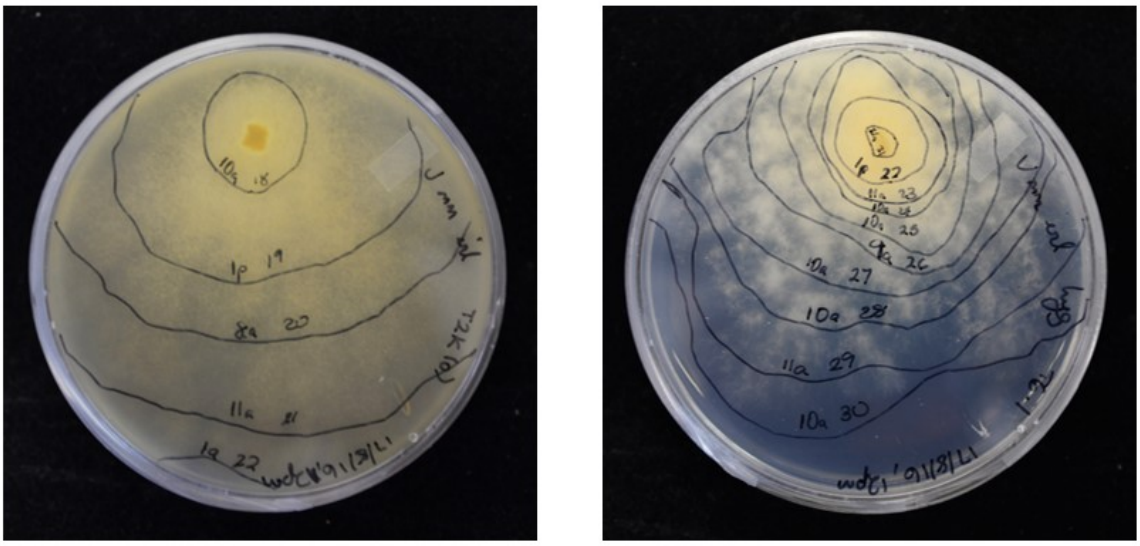

Figure 14. Images showing growth phenotype of (a) T2k(0) and (b) T6.1. Solid lines indicate time intervals of ~24 hours. T2k(0) displays suppression of *un-24*^{PA}*het-6*^{OR} incompatibility. T6.1 displays partial suppression of incompatibility associated with the ectopic *het-6*^{OR}. Strains were grown on Vogel's minimal medium with inositol; T6.1 was grown on medium also containing 200µg/mL hygromycin B. Strains were incubated at 30°C.

PCR-mediated deletion of vib-1 binding site

The PCR-mediated deletion of the putative DNA binding site of VIB-1was confirmed using a diagnostic PCR, and subsequently with sequencing (Figure 16). Primer pair pCOR1vd1Afw + pCOR1vd1rv amplified both pCOR1 and pCOR1vd across the VIB-1 binding site. However, pCOR1vd1Bfw + pCOR1vd1rv only amplified across the deletion

(a)

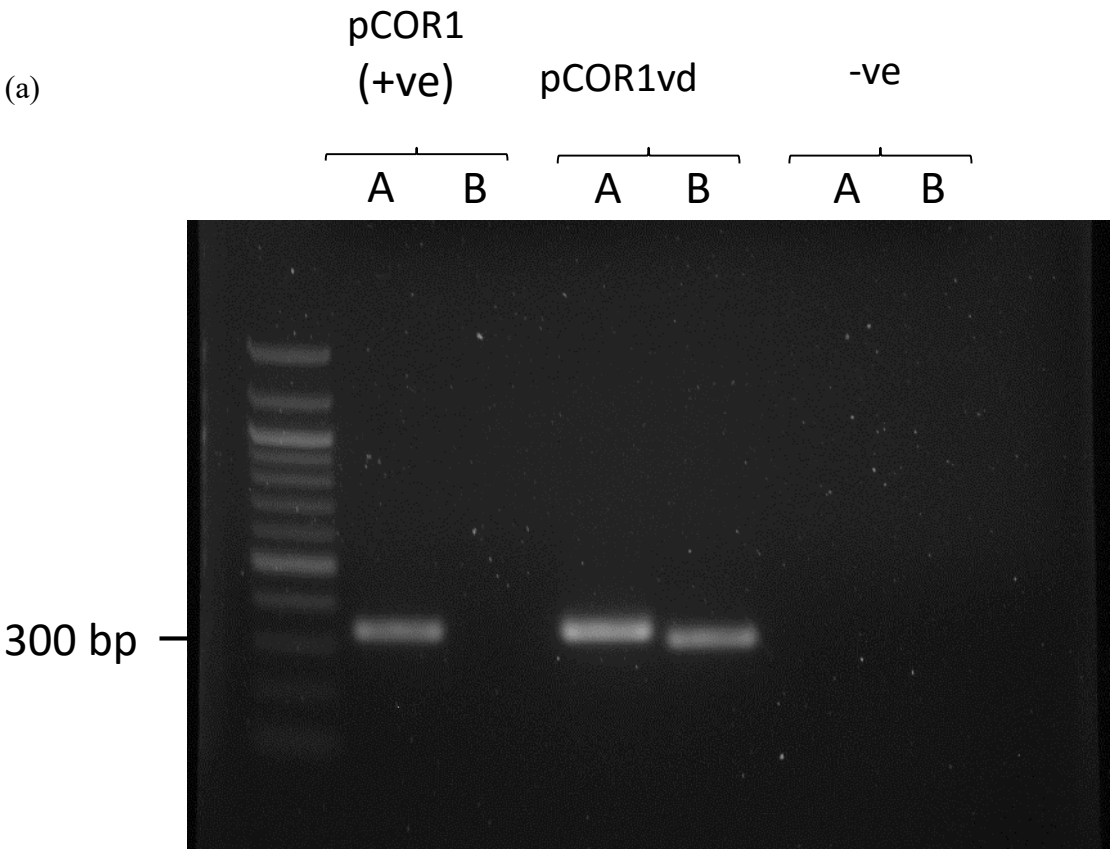

(b)

VIB-1 binding site

```
Nchet-6OR     TGCTTGCCTAGCCAATCACACGCCATTTTACCTCGTCATGTAGGTAACCTCGCCATGTAA
pCOR1vd       TGCTTGCC------GTACGACGCCATTTTACCTCGTCATGTAGGTAACCTCGCCATGTAA
              *******      *  ****************************************

Nchet-6OR     CCTCAACATGTGATCCTAGCGTCGATGGCCTCTTGGGTTCAGGTCAGGCAGCCATATTCG
pCOR1vd       CCTCAACATGTGATCCTAGCGTCGATGGCCTCTTGGGTTCAGGTCAGGCAGCCATATTCG
              ************************************************************
```

Figure 15. Confirmation of VIB-1 binding site deletion construct. (a) 1% agarose gel showing electrophoresis of diagnostic PCR to confirm the VIB-1 binding site deletion construct. Letters above lanes indicate which diagnostic forward primer was used in the PCR reaction mix; A= pCOR1vd1Afw + pCOR1vd1rv, B= pCOR1vd1Bfw + pCOR1vd1rv (Table 3). (b) Sequence alignment of the *het-6*^{OR} sequence with the pCOR1vd deletion construct. The VIB-1 binding site in the wild-type sequence (top) is indicated by a red box, while the *Bsi*WI restriction site is indicated by the yellow highlight.

construct in pCOR1vd (Figure 16(a)). Figure 16(b) shows sequencing data that confirms that the VIB-1 binding site was successfully replaced with the *Bsi*WI restriction site (Appendix B).

A single transformant, designated as T5VD, was observed to display a Type II-like growth pattern. Levene's test indicated that the variance between the control cohort and the T5VD cohort was equal ($p = 0.82$; $\alpha = 0.05$). An unpaired Student's t-test indicated that the average growth rate of the T5VD transformant (0.4 ± 0.21 mm/hr) was significantly lower than the control strain (0.66 ± 0.014 mm/hr) ($df = 177$; $p < 0.001$). Interestingly, this transformant also displayed a loss of conidiation as observed in the control strain. Figure 16 summarizes the growth rates of othe control and T5VD cohorts, while figure 17 shows images of replicate plates of these strains

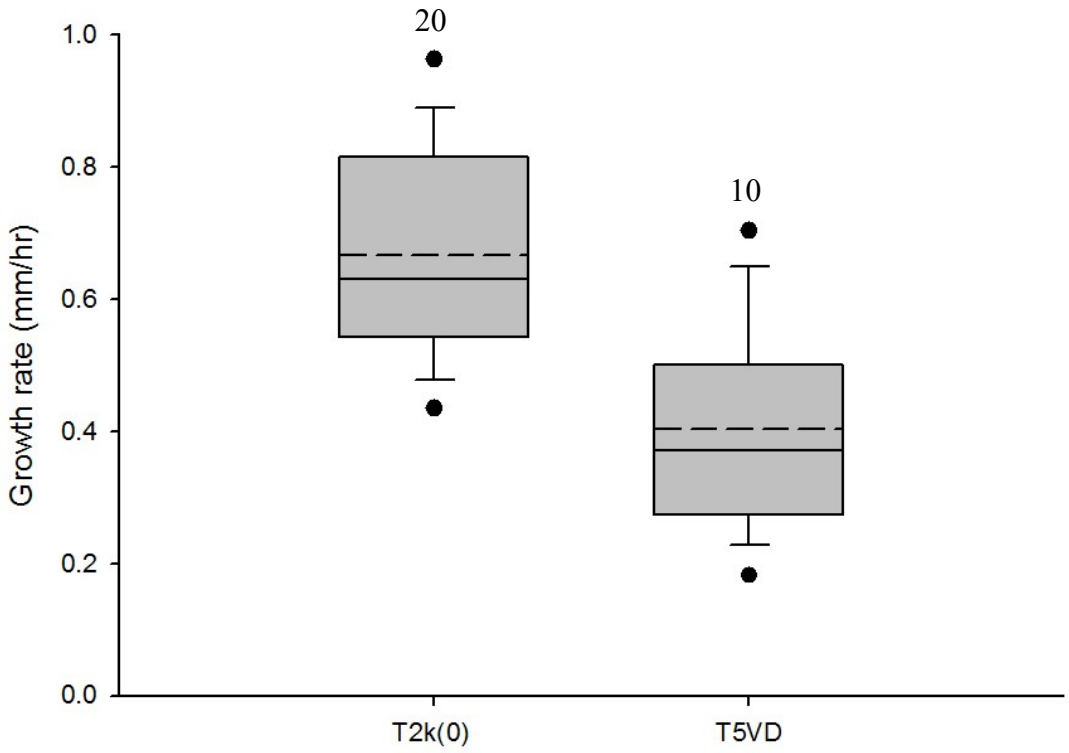

Figure 16. Box plots representing the growth rates of a Type II escape strain (T2k(0)) and a transformant strain bearing the pCOR1vd construct (T5VD). The black dotted lines in the box plots indicate the mean growth rate for each cohort, solid lines inside the box represent the median growth rate. Whiskers indicate 5th and 95th percentiles respectively; outliers are represented by solid dots. Numbers above box plots indicates the number of replicates in each cohort. Comparison of means was by unpaired Student's t-test ($\alpha = 0.05$)

(a) (b)

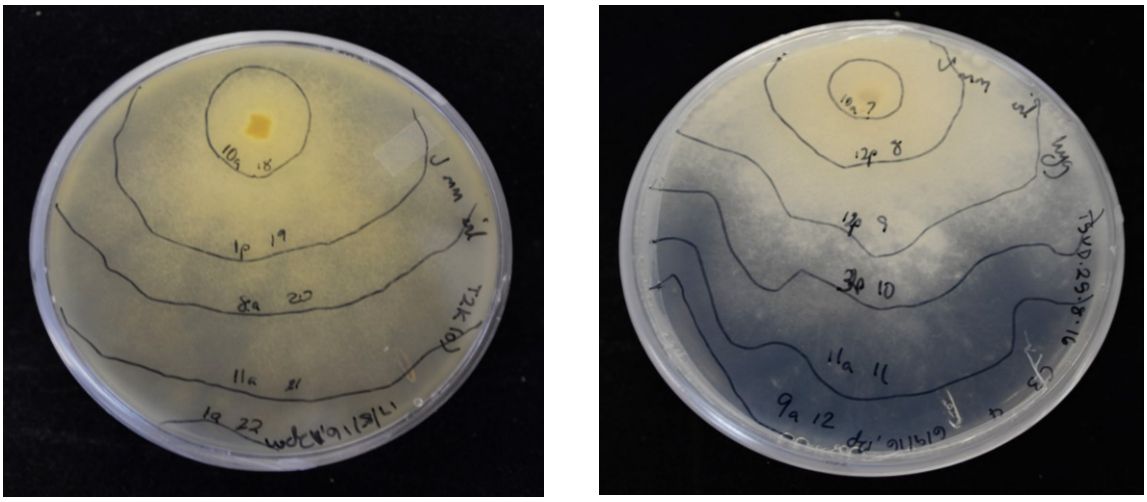

Figure 17. Images showing growth phenotype of (a) T2k(0) and (b) T5VD. Solid lines indicate time intervals of ~24 hours. T2k(0) displays suppression of *un-24*^{PA}*het-6*^{OR} incompatibility. T5VD displays a phenotype that is similar to a Type II escape. Strains were grown on Vogel's minimal medium with inositol; T5VD was grown on medium also containing 200µg/mL hygromycin B. Strains were incubated at 30°C.

Overall, the growth rate of pre-escape strains of both DLL 14-1 and the T5 transformants were the slowest observed in this study. The fastest growth rates observed were associated with post-escape growth in both DLL 14-1 and T5, but the DLL 14-1 post-escape growth was more similar to a WT strain in magnitude and variance. T2k(0), which is a strain that underwent Type II escape, had growth rates that were intermediate between the pre- and post-escape growth rates. The T6 transformants displayed growth rates that were faster than pre-escape growth rates, but slower than Type II growth rates. Similarly, the T5VD transformant displayed growth rates that were faster than pre-escape growth but slower than the Type II control. Figure 18 summarizes these observations.

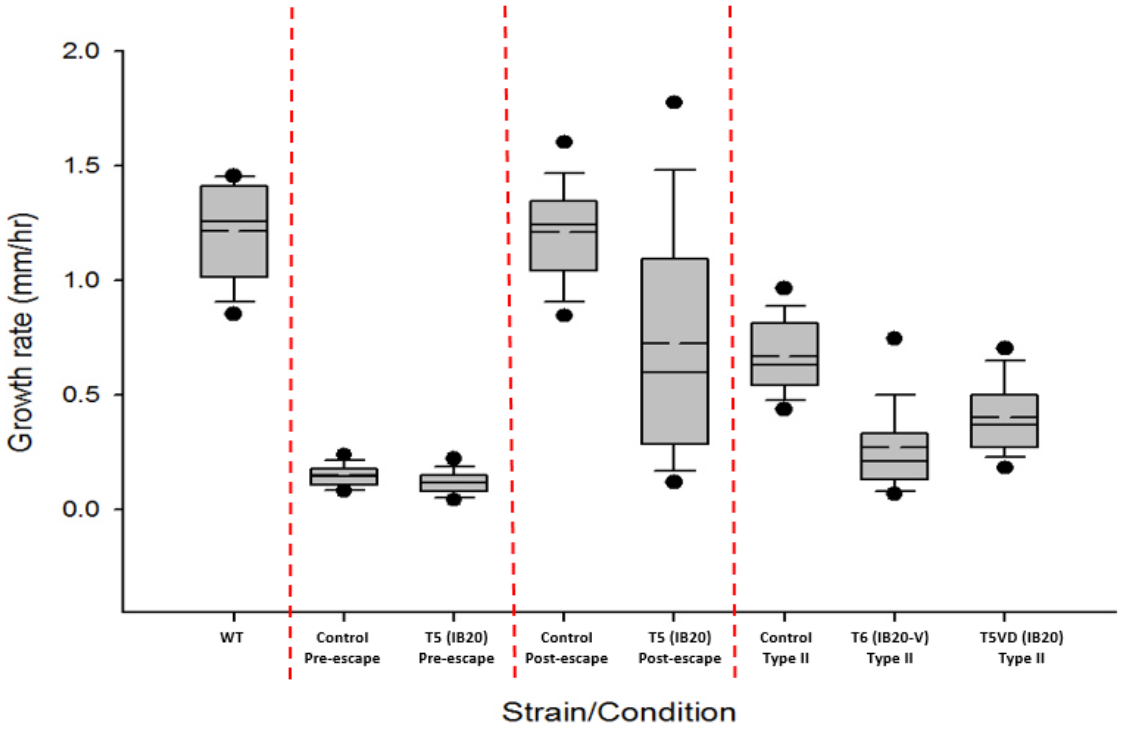

Figure 18. Box plots summarizing the observed growth rates of different strains used in this study. WT growth rates were obtained from DLL 8-16, which lacks incompatibility because the endogenous *het-6*^{OR} is replaced with the *hph* gene. Pre- and post-escape growth rates are shown for the SI strains DLL 14-1 (control) and T5 (IB20 transformed with pCOR1). Daily growth rates are also shown for T2k(0) (Type II escape strain), T6 (IB20-V transformed with pCOR1), and T5VD (IB20 transformed with pCOR1vd). The black dotted lines in the box plots indicate the mean growth rate for each cohort, solid lines inside the box represent the median growth rate. Whiskers indicate 5th and 95th percentiles respectively; outliers are represented by solid dots.

Discussion

This study examined the role of the promoter region of the *het-6*^{OR} gene in mediating escape from self-incompatibility. We introduced an ectopic copy of the *het-6*^{OR} gene into a strain of *N. crassa* bearing a partial knockout of the endogenous *het-6*^{OR} (-555 to +324). It could thus be assumed that any incompatibility phenotype observed in these transformants could only be attributed to the ectopic *het-6*^{OR}. 5 transformant colonies that exhibited self-incompatibility were identified, indicating that the ectopic *het-6*^{OR} is capable of participating in a nonallelic interaction with *un-24*^{PA} to confer incompatibility. Evidence from previous studies suggests that HI is mediated by protein-protein interactions between incompatibility factors (Dos Reis *et al*., 2002; Sarkar *et al*., 2002; Reshke, 2013). In this study, the presence of an ectopic *het-6*^{OR} allele was sufficient to induce self-incompatibility in independent transformant strains, despite the fact that the ectopic *het-6*^{OR} in each of these transformants was randomly inserted into the genome. The most parsimonious inference from these observations is that the interaction between UN-24^{PA} and the ectopic HET-6^{OR} leads to self-incompatibility in transformant strains. These results provide further evidence in support of the protein-protein interaction model of HI.

Escape has been associated with a range of processes, including large deletions, chromosomal rearrangements, ectopic recombination, and point mutation (Smith *et al*., 1996; Chevanne *et al*., 2010). There is some evidence to suggest that escape from vegetative incompatibility is mediated by directed mutation of specific incompatibility genes (Chevanne *et al*., 2010; Lafontaine and Smith, 2012), as opposed to random mutagenesis. This study sought to test whether directed mutation or random mutagenesis

is at play during escape by observing escape in transformant strains bearing an ectopic *het-6*^{OR}. In the event that random mutagenesis is responsible for initiating escape, the expectation is that escape frequency and timing would be similar in the DLL 14-1 strain and translocation construct used in this study. However, the results of this study indicate that there is a difference in escape associated with the presence of the endogenous *het-6* and the ectopic transgene.

Given that the introduction of the ectopic *het-6*^{OR} into IB20 involved random insertion into the genome, it was expected that there would be some variation in the behavior of resulting self-incompatible strains as a result of the context of the ectopic insertion. While there was variation in average escape time between the DLL 14-1 strain and the five transformant cohorts studied, there was also significant variation in escape times within the transformant cohorts (Figure 9). In the DLL 14-1 cohort, escape time occurred within a range of 1.4 – 5.8 days. In contrast, escape times observed among the transformant cohorts ranged between 3 – 17.6 days. The average time to initiate escape was also significantly increased in the transformant cohorts. The DLL 14-1 cohort had an average escape time of 4.3 ± 0.14 days, which is consistent with observations by Lafontaine and Smith (2012). On the other hand, the average escape time of the transformant cohorts ranged from 6.5 ± 1.15 days to 12.1 ± 1.05 days. Taken together, the results from this study suggest that escape in the DLL 14-1 strain is more tightly regulated than in the transformant strains. In IB20, the large deletion that renders the *het-6*^{OR} gene non-functional potentially disrupts the promoter region. Thus, it can be inferred that the promoter region of the *het-6*^{OR} gene plays a role in regulating escape via mutation in the endogenous *het-6*.

One possibility is that the promoter region acts as a target for mutational machinery during

incompatibility, such that the *het-6* gene is more likely to undergo a mutation that initiates escape. However, since the promoter region of *het-6* in IB20 is disrupted, this targeting mechanism is lost in transformants experiencing self-incompatibility due to the ectopic *het-6*^{OR}. As a result, mutations that alter the ectopic *het-6*^{OR} and induce escape are more likely to be the introduced by random mutation. This is supported by the fact that variance in escape time among replicates of the same transformant cohort was high. For example, escape times for cohort T5.2 ranged between 4.7 – 17.6 days.

The pre-escape and post-escape behaviors of transformant cohorts were also compared to the DLL 14-1 strain. There was a slight but statistically significant decrease in the pre-escape growth rate of some of the transformant cohorts (Figure 11a). The DLL 14-1 strain exhibited an average pre-escape growth rate of $0.14 \pm 6.8 \times 10^{-3}$ mm/hr, which was similar to the rate for T5.1 (0.14 ± 0.021 mm/hr) and T5.3 (0.14 ± 0.018 mm/hr). This differed from the average pre-escape growth rates of T5.2 (0.12 ± 0.016 mm/hr), T5.4 (0.087 ± 0.015 mm/hr), and T5.5 (0.12 ± 0.01 mm/hr). The use of random ectopic insertion in this study makes it difficult to ascertain how much of this decrease in pre-escape growth rate is attributable to insertion context effects.

Comparison of the post-escape growth rates did reveal some interesting trends (Figure 11b). The DLL 14-1 strain had an average post escape growth rate of (1.21 ± 0.029 mm/hr), and following escape, post-escape growth rates remained consistently above the threshold of 0.3 mm/hr; the minimum post-escape growth rate for the DLL 14-1 cohort was 0.83 mm/hr. Two of the transformant cohorts, T5.1 and T5.3, exhibited average post-escape growth rates that were similar to the DLL 14-1 strain (1.12 ± 0.24 mm/hr and 1.08 ± 0.19 mm/hr), but other cohorts displayed significantly decreased average growth rates, ranging

from 0.47 ± 0.16 mm/hr (T5.3) to 0.71 ± 0.14 mm/hr (T5.2). Much of this decrease in average post-escape growth rate could be attributed to the fact that some transformant replicates displayed pre-escape-like growth after the escape sector had emerged from the colony (Figure 12). Of the 43 replicates that underwent escape, 12 replicates had post-escape growth rates lower than 0.3 mm/hr. In some instances, post-escape growth rates as low as 0.125 mm/hr were recorded. This could indicate that the mechanism mediating escape in the transformant cohorts is not a permanent change, as seen in the DLL 14-1 strain.

Three kinds of gene silencing mechanisms have been observed in fungi – repeat-induced point mutation (RIP), methylation induced premeiotically (MIP), and quelling (Irelan and Selker, 1996). RIP occurs during the sexual cycle of *N. crassa*, and causes duplicated DNA sequences, whether endogenous or ectopic to be subjected to a high frequency of mutation. Sequences subjected to RIP display transition mutations and, in some instances, heavy cytosine methylation. This process is highly efficient, and duplicated sequences remain sensitive to RIP over multiple generation, although sensitivity decreases as cumulative mutations reduce the homology between the sequences (Cambareri *et al*., 1991). MIP is found in *Ascobolus immersus*, and similar to RIP, occurs during the sexual cycle. Unlike RIP, gene silencing by MIP is the result of cytosine methylation and not point mutations. The epimutation associated with MIP is also heritable in a Mendelian fashion (Rhounim *et al*., 1992). Quelling is a form of post-transcriptional gene silencing found in *N. crassa* that is associated with the vegetative growth phase, making it distinct from RIP and MIP. Like RIP and MIP, quelling is triggered by the presence of duplicated sequences, and it affects both sequences that are endogenous to the *N. crassa* genome and foreign genes (Romano

and Macino, 1992; Pandit and Russo, 1992). Transgenes that undergo quelling display heavy cytosine methylation, but Cogoni *et al*. (1996) demonstrated that while methylation may be necessary for quelling, it is not sufficient to cause it. Quelling can be triggered by fragments of transgenes (~132 nt), but the process is reversible, and duplication-bearing transformants may revert completely or partially to a pre-quelling phenotype (Romano and Macino, 1992; Pandit and Russo, 1992; Cogoni *et al*., 1996).

Quelling was first identified during experiments involving the overexpression of albino-3 (*al-3*), a gene involved in the synthesis of carotenoids that contribute to the bright orange color of wt *N. crassa*. Surprisingly, ~36% of transformant strains displayed an albino phenotype. There were no DNA rearrangements associated with the endogenous gene, and there was no correlation between copy number and the albino phenotype. There was, however, a significant reduction in the level of steady state mRNA of the genes duplicated by transformation. These observations indicated that the presence of the transgene acted as the trigger for a post-transcriptional gene silencing (PTGS) mechanism that could co-suppress the expression of the endogenous copy of the gene (Cogoni *et al*., 1994).

Cogoni *et al*. (1996) demonstrated that in a heterokaryon, quelling is a dominant trait and acts in *trans*, implicating a diffusible molecule like RNA in the gene silencing. Strains of *N. crassa* that experience quelling display an accumulation of short (21-25 nt) sense and antisense RNA fragments, which is consistent with the occurrence of RNA intermediates in other eukaryotic PTGS mechanisms. The presence of both orientations of the RNA fragments suggested that an important step in the triggering of quelling is the formation of double stranded RNA (dsRNA) (Catalanotta *et al*., 2002). Genetic screening identified three loci that are essential for quelling, *qde-1, -2*, and *-3* (Cogoni and Macino, 1997). *qde-*

1 and *qde-3* seem to have a role in the generation of the dsRNAs that are associated with PTGS. QDE-1 is a homolog of RNA-dependent RNA polymerase (RdRP), and catalyzes RNA-dependent RNA polymerization on single stranded RNA (ssRNA) templates, while *qde-3* encodes a DNA helicase. Experimental evidence suggests that QDE-1 is required for the recognition and processing of transgenic ssRNAs into dsRNA prior to quelling. QDE-1 also displays DNA-dependent RNA polymerase (DdRP) activity and has been implicated in the generation of aberrant RNA (aRNA) from transgenic loci (Catalanotta *et al*., 2002; Makeyev and Bamford, 2002; Lee *et al*., 2010; reviewed in Dang *et al*., 2011). Other RdRPs have been shown to be essential for PTGS in plants (Mourrain *et al*., 2000). *qde-2* encodes a homolog of Argonaute 2 (AGO2), a protein found in *D. melanogaster*. AGO2 is a component of the RISC multiprotein complex that plays a significant role in RNA interference (RNAi), another form of dsRNA-induced gene silencing. AGO2 shares a PAZ domain with Dicer, another RISC complex protein. The PAZ domain is thought to be important for protein-protein interaction between AGO2 and Dicer that facilitates the incorporation of siRNAs into RISC and the subsequent targeting of cognate mRNAs from duplicated sequences (Bernstein *et al*., 2001; Catalanotta *et al*., 2002).

Quelling is thought to proceed in the following way. First, aRNAs are generated from a ssDNA template of a repetitive transgene locus (usually tandemly repeating) by QDE-1, and processed into dsRNA. These dsRNAs are recognized by QDE-3 and then cleaved by Dicer-like proteins (DCL1 and DCL2) into ~25nt siRNA duplexes. QDE-2 loads the siRNA duplex into RISC, and cleaves one strand of the duplex to allow proper targeting of mRNA. QDE-2 recruits an exonuclease, QIP, to degrade the unused passenger strand. This cleavage may act as the trigger for the initiation of target RNA degradation by RISC. The

result is the post-transcriptional silencing of both the repetitive transgenic loci and the corresponding endogenous locus, leading to a phenotype more characteristic of a deletion mutant (Bernstein *et al*., 2001; reviewed in Dang *et al*., 2011).

Quelling is a reversible process, as evidenced by the instability of the albino phenotype in the above study. Over time, the quelled transformants reverted to a wildtype or near-wildtype phenotype (Cogoni *et al.*, 1994). Reversible inactivation is thought to be regulated in part by the number of ectopic insertions and the presence of sustained stress. For instance, following transformation with a hygromycin resistance gene, Pandit and Russo (1992) generated conidial stocks of Hyg^R transformants cultured in the presence and absence of Hyg, and observed greater colony forming units (CFUs) when conidia obtained from +Hyg stocks were grown on media containing hyg. They determined that the difference in CFUs between the conidial stocks was not due to physical instability of the ectopic inserts, which were stable over 25 mitotic divisions. They compared the ratio of Hyg^R conidia that were grown from the +Hyg and –Hyg conidial stocks as a measure of the reversibility of the *hph* gene, a value they refer to as the 'inactivation factor'. Reversible inactivation tended to occur in transformants that had ≥3 insertion sites, and these transformants displayed relatively high inactivation factors (Table 2 in Pandit and Russo, 1992). Romano and Macino (1992) found that reversion was associated with loss of the exogenous copies of the duplicated sequence, while Pandit and Russo (1992) did not observe any loss of the duplicated sequence. Furthermore, Pandit and Russo (1992) observed that the reactivated genes were susceptible to re-silencing.

The traits of the quelling mechanism make it an interesting candidate for the irregular escape behavior observed in the ectopic *het-6*^{OR} transformants, in particular the reversion

to pre-escape growth rate following escape. The transformants used in this study were maintained on a medium containing Hyg to sustain selection for the *hph* gene in pCOR1. If the hypothesis that sustained stress contributes to reversible inactivation is correct, it may provide an explanation for the restoration of the self-incompatible phenotype in ectopic *het-6*^{OR} transformants. Assuming that reversible inactivation is correlated with high ectopic insertion and sustained stress, and that transgenes are stable in the genome over multiple mitotic divisions, the following scenario could explain the aberrant post-escape phenotype: the presence of ectopic *het-6*^{OR} triggers quelling, which silences the transgene and abolishes self-incompatibility, permitting escape. Sustained growth of the transformants in the presence of Hyg promotes reversible inactivation of the transgene, which is then able to engage in a nonallelic interaction with *un-24*^{PA}, restoring self-incompatibility.

The results of this study suggest the following:

(i) The ectopic *het-6*^{OR} undergoes a nonallelic interaction with the endogenous *un-24*^{PA} in IB20 resulting in an SI phenotype, which indicates that protein-protein interactions between UN-24^{PA} and HET-6^{OR} precede the incompatibility.

(ii) Escape in DLL 14-1 (control) is more tightly regulated than in the ectopic *het-6*^{OR} transformants, and the *het-6*^{OR} promoter region may play a role in this targeting mechanism

(iii) Escape in these ectopic *het-6*^{OR} transformants is more likely the result of random mutagenesis, as evidenced by the high variance in escape time within transformant cohorts.

(iv) A small portion of transformant replicates (~28% in this study) may have

undergone escape via PTGS by quelling.

(v) Some quelled replicates experience reversible inactivation, restoring the self-incompatibility imbued by the ectopic *het-6*^{OR}. This is observed as a reversion to pre-escape growth rate following the emergence of the escape sector.

The transformation of IB20-V with pCOR1 generated four transformants that behaved similarly to the DLL T2k(0) control strain. These transformants exhibited growth rates that were faster than SI colonies, but slower than wild type colonies. However, it is of interest to note that the transformant cohorts also exhibited brief periods of extremely slow growth (< 0.1 mm/hr), followed by growth rates that were more typical of Type II strains (Figure 13). Furthermore, in general, the average growth rates of the transformant cohorts was slower when compared to DLL T2k(0). These results indicate that there was some suppression of incompatibility between the ectopic *het-6*^{OR} and *un-24*^{PA}, but this suppression was not as strong as that observed in DLL T2k(0). This suppression of HI is consistent with observations made by Smith and Lafontaine (2012). However, the variation in growth rates among transformant cohorts may be the result of context effects associated with the insertion point of the ectopic *het-6*^{OR}. Lafontaine and Smith (2012) also showed that VIB-1 suppresses *un-24*^{PA}*het-6*^{OR} incompatibility by negatively regulating *het-6*^{OR} transcription, whereas the partial suppression of *un-24*^{OR}*het-6*^{PA} incompatibility was by some mechanism other than the negative regulation of transcription. An interesting question for future studies would be whether the suppression of the ectopic *het-6*^{OR} is accomplished by the negative regulation of transcription or by the second unknown mechanism.

The pCOR1vd plasmid constructed in this study was derived from pCOR1, and

eliminated the putative VIB-1^{+} binding site in the upstream region of *het-6*^{OR} by replacing it with the restriction site sequence for the *Bsi*WI endonuclease (Figure 15). The T5VD transformant was obtained by transforming IB20 with the pCOR1vd construct, and this transformant displayed a Type II-like phenotype, including feathery hyphae and repressed conidiation. This result was expected, as the pCOR1vd construct replicates the negative regulation of transcription of the ectopic *het-6*^{OR} observed in a typical Type II escape. However, the average growth rate of T5VD was significantly lower than the control Type II strain, indicating that the ectopic *het-6*^{OR} is not suppressed to the same degree as the endogenous *het-6*^{OR} in the control. Further experiments with this construct may provide more insight into the role of *vib-1* in the suppression of incompatibility at the *het-6* locus.

This study has provided novel insights into HI at the *het-6* locus. HI in *N. crassa* displays features similar to nonself recognition in higher eukaryotes, and a more thorough understanding of this phenomenon provides a unique perspective on the nature of nonself recognition across many species, including humans. The *het-6* locus in particular is of interest because the HET-6 protein has no known function outside of HI, and this has made it difficult to determine the underlying mechanism behind the interaction between *un-24* and *het-6*. The current hypothesis is that one allelic variant of HET-6 undergoes a protein-protein interaction with the opposing variant of UN-24, but it is unclear whether the resulting complex acts as a trigger for PCD pathways (via the HET domain of HET-6) or is itself toxic to the cell. The results of the ectopic *het-6*^{OR} construct provide further evidence in support of the protein-protein interaction hypothesis, but the exact end point of this interaction warrants further investigation. We also demonstrated that the upstream

promoter region of *het-6*^{OR} plays a role in regulating the initiation of escape by mediating preferential targeting of *het-6*^{OR} for mutation. In addition, we showed that a mutation in *vib-1* is able to suppress HI associated with the ectopic *het-6*^{OR}, although the mechanism underlying this suppression occurs is still unclear. Finally, we generated a plasmid construct in which the putative VIB-1^{+} binding site upstream of *het-6*^{OR} was deleted. Transformation of the partial knockout strain with this construct generated a transformant that displayed a Type II-like phenotype. This VIB-1^{+} binding site deletion construct presents a useful study for future studies.

Appendix A

Sequence alignment of the *het-6* locus in IB20 and the wt *het-6*^{OR} sequence. The large 877 bp deletion that resulted in escape from self-incompatibility is shown. The *het-6*^{OR} start and stop codons are also indicated.

```
IB20          -------------------------CCATCGGTCCTGCTTTTCACACAACACCCGAGGCC
Nchet-6OR     -ACGTACCTTCCCCGGTCTTTTTGGCCATCGCTCCTGCTCTTCACACAACACCCGAGGCC

IB20          GAAGGTGCTAATCACATAACCTGGAAAGCGGCCTGAAATTACAGATAGAGAGGACCGCCC
Nchet-6OR     GAAGGTGCTAATCACATAACCTGGAAAGCGGCCTGAAATTACAGATAGAGAGGACCGCCC

IB20          GGAAAAGTTCGGGCCATGCGCTTTGTTCTTCATACAAAAAAAGAAAAAAGAAATAAAAAA
Nchet-6OR     GGAAAAGTTCGGGCCATGCGCTCTGTTCTTCATACAAAAAAAGAAAAAAGAAATAAAAAA

IB20          AAAATAAAAAAAAAGGAAAAGGAAAATTGAAAATTCAAAAAGAAAAGCACAAAGACACGA
Nchet-6OR     AAAATAAAAAAAAAGGAAAAGGAAAATTGAAAATTCAAAAAGAAAAGCACAAAGACACGA

IB20          CTCACCGAAAAACATTGAGTTCCTAGAAAGGGCTCAGGAATTGTCCACCCAGTCTATTGC
Nchet-6OR     CTCACCGAAAAACATTGAGTTCCTAGAAAGGGCTCAGGAATTGTCCACCCAGTCTATTGC

IB20          CCAGGATGTCCTTCAGTTTCGTCCGCATAATCCACAACTGCGCAATTGCCAAGGGGAACC
Nchet-6OR     CCAGGATGTCCTTCAGTTTCGTCCGCATAATCCACAACTGCGCAATTGCCAAGGGGAACC

IB20          TGTCTTGTTTATTTGGGGCAATCTCTCTCACACGACTTTTTTCTTCCTTT-CTTCCTCTTC
Nchet-6OR     TGTCTTGTTTATTTGGGGCAATCTCTCTCACACGACTTTTTTCTTCCTTTTCTTCCTCTTC

IB20          AACTT-----------------------------------------------------
Nchet-6OR     AACTTCAGCAGAACATGTTGTTTGGTAATGAAGAGATCTGGGTCAGAATTCAGGCCGCTT

IB20          -----------------------------------------------------------
Nchet-6OR     TTTCTCTCAAAGCTACTATTCTTGCTCTTCATGATGTCCTTCTTTTCCCATGTCTGTCTT

IB20          -----------------------------------------------------------
Nchet-6OR     CCTTCATACTCTTCGCCCCTATTATCCACCTCCCTCCGATATCCTTCGATCTACTTTCTC

IB20          -----------------------------------------------------------
Nchet-6OR     TTCTTTGCCCATTTCCTCTTCGTCCTCCTACTACTCAGTTCTCCCACATAATGCTACATG

IB20          -----------------------------------------------------------
Nchet-6OR     GCTATGCTCCTTTCCTACGGCGATAGCCACAAGATCCAACCATGTTGGAGGTTTTCTCAG

IB20          -----------------------------------------------------------
Nchet-6OR     CTCAGGGCCCTGCTTGCCTAGCCAATCACACGCCATTTTACCTCGTCATGTAGGTAACCT
```

```
IB20          ------------------------------------------------------------
Nchet-6OR     CGCCATGTAACCTCAACATGTGATCCTAGCGTCGATGGCCTCTTGGGTTCAGGTCAGGCA

IB20          ------------------------------------------------------------
Nchet-6OR     GCCATATTCGATGGATCTCCAGCCTCATCTCAAATTTCCAACATCATCGAGCTTGCAGCA

IB20          ------------------------------------------------------------
Nchet-6OR     GCCGCTTTTCTTGGAATTGTTGCCATTGATCCTACTTGCCTATCATTTGATGTCGTGCGC

IB20          ------------------------------------------------------------
Nchet-6OR     CGTCCGATCTCTTCGTCTTCATGGCTAATTCCGCGCAGACGGACACAGTGTCGGCCGGTA
                                  START

IB20          ------------------------------------------------------------
Nchet-6OR     ACCTGTTCAGCTATGACTCGGTTGCTCTGTCAGATCCGTCAACCCACATTCGTCTGCTTG

IB20          ------------------------------------------------------------
Nchet-6OR     ACCTCCATCCCGCTTCTTGTTATACGGACGACCTATACTGCTGCATATACACTGCGCCGA

IB20          ------------------------------------------------------------
Nchet-6OR     TTTCGCCGCCGCCCAGCTATATCGCACTTTCATACGTCTGGGGGGGATAGCACCAGGACGC

IB20          ------------------------------------------------------------
Nchet-6OR     ATGAGATTTCAGTGGCCAATGAAGTCAACGATGGCAGAGCTTTTATACCACTACGCCTGA

IB20          ------------------------------------------TACCGGCGGCAGCTTG
Nchet-6OR     CATCATCCCTGGATACTTGCCTCCGTCATCTTCGAGAACTCCATTACCGGCGGCAGCTTG

IB20          AGCCTCTGCCTCTATGGATTGACCAGATATGTATCAATCAGGACGACAACGAGGAAAAGT
Nchet-6OR     AGCCTCTGCCTCTATGGATTGACCAGATATGTATCAATCAGGACGACAACGAGGAAAAGT

IB20          CCTTCCAGGTCCGGCTCATGAGGGATATCTACTCGTCAGCCCACCAAGTCGTCGTGTGGC
Nchet-6OR     CCTTCCAGGTCCGGCTCATGAGGGATATCTACTCGTCAGCCCACCAAGTCGTCGTGTGGC

IB20          TAGGACCTGCTGTTGACGACTCCAACAGAGTGATGGATGCCTTGGCAGAAGTTGGTCAAG
Nchet-6OR     TAGGACCTGCTGTTGACGACTCCAACAGAGTGATGGATGCCTTGGCAGAAGTTGGTCAAG

IB20          AATTCCTCGATAAGATCGGCGATCATACCGAAGAAGAACATTGGCTTTCCGTCGATCGCC
Nchet-6OR     AATTCCTCGATAAGATCGGCGATCATACCGAAGAAGAACATTGGCTTTCCGTCGATCGCC

IB20          TCATCAAGGAAAAGATTGAACAACCTGATGCCGTTACTTTCTTGCGTGAGGCATACAAGG
Nchet-6OR     TCATCAAGGAAAAGATTGAACAACCTGATGCCGTTACTTTCTTGCGTGAGGCATACAAGG

IB20          TTATCTATATGCTAAACAGAGAACACTCTTTTACACGTTGGGTGGAAAGAACATGGTTCA
Nchet-6OR     TTATCTATATGCTAAACAGAGAACACTCTTTTACACGTTGGGTGGAAAGAACATGGTTCA

IB20          AGCGACTGTGGACTATACAGGAATTCTGTCTCTGTGCAGATACGATTTTCGCTTGTGGTT
Nchet-6OR     AGCGACTGTGGACTATACAGGAATTCTGTCTCTGTGCAGATACGATTTTCGCTTGTGGTT
```

```
IB20          ACAAGGTTGTCTCTCAGAAAATGGTCTCCGCACTGACCGATTTTATGAGATGCATTATCA
Nchet-6OR     ACAAGGTTGTCTCTCAGAAAATGGTCTCCGCACTGACCGATTTTATGAGATGCATTATCA

IB20          TGGACAAATGTTTGCGGGGACTTCTGGAGACCCCTGACACACCTACATATTCCACCCTCT
Nchet-6OR     TGGACAAATGTTTGCGGGGACTTCTGGAGACCCCTGACACACCTACATATTCCACCCTCT

IB20          TCTCAGGGCTCATGAGATTATTCCCGCTCTTTCAGCATCGGGGGTACTGCCAGTACCCGT
Nchet-6OR     TCTCAGGGCTCATGAGATTATTCCCGCTCTTTCAGCATCGGGGGTACTGCCAGTACCCGT

IB20          ATCGGAAAGAGACACTGGAACACCTCCTTGTAGAACTCTTTGTGGGAGTCACACCGCCAT
Nchet-6OR     ATCGGAAAGAGACACTGGAACACCTCCTTGTAGAACTCTTTGTGGGAGTCACACCGCCAT

IB20          GCGTTACCAATAAGCGCGACAAAGTGTATGGACTCCTTGGCTTAGCGGGGGACGCCGATG
Nchet-6OR     GCGTTACCAATAAGCGCGACAAAGTGTATGGACTCCTTGGCTTAGCGGGGGACGCCGATG

IB20          AACTTGGTATTCGGCCGGATTATACTACGTCGACGACCCTTGCGCAAGTGTTTACACAAA
Nchet-6OR     AACTTGGTATTCGGCCGGATTATACTACGTCGACGACCCTTGCGCAAGTGTTTACACAAA

IB20          CAGCAAGAGCGATAATCCAAAAGAACTGGAAAATTCAGCGAAAGAGAGGTCTACAAATCC
Nchet-6OR     CAGCAAGAGCGATAATCCAAAAGAACTGGAAAATTCAGCGAAAGAGAGGTCTACAAATCC

IB20          TTCGCTATGGGAGCTTAGGACAAAGGAAATCTGCCCCCAAGAATGAGACGGATTTACCGT
Nchet-6OR     TTCGCTATGGGAGCTTAGGACAAAGGAAATCTGCCCCCAAGAATGAGACGGATTTACCGT

IB20          CATGGGTGCCTGAGTGGAACGGCAGGATCGCCAAGACTTATCAGCGAGAGATGTCATTCT
Nchet-6OR     CATGGGTGCCTGAGTGGAACGGCAGGATCGCCAAGACTTATCAGCGAGAGATGTCATTCT

IB20          TAGCTTGTGGGGAGATCAGAATGCCGGATTTGGTGCCAACTACATCCCCTACGATTCTGG
Nchet-6OR     TAGCTTGTGGGGAGATCAGAATGCCGGATTTGGTGCCAACTACATCCCCTACGATTCTGG

IB20          GCCTCCGCGGTTTTTGCGTGGGTACTATCGTAGATCTAGGAGAGCAGGCACGGGTGGACA
Nchet-6OR     GCCTCCGCGGTTTTTGCGTGGGTACTATCGTAGATCTAGGAGAGCAGGCACGGGTGGACA

IB20          TTTGGCGGCGTTCTGCTGACGGTGCCAAGAAAATCGTTGGATTTTTCGACAACTTCAGGA
Nchet-6OR     TTTGGCGGCGTTCTGCTGACGGTGCCAAGAAAATCGTTGGATTTTTCGACAACTTCAGGA

IB20          GACTTTTGAACTTGTCCAAGCAGAACAAGCGTGCTAAGGACATCTATGCAAGTACTGCTC
Nchet-6OR     GACTTTTGAACTTGTCCAAGCAGAACAAGCGTGCTAAGGACATCTATGCAAGTACTGCTC

IB20          ATCATGATGCTGCCCTATGGCGAGTGCCCATTGGTGATCAGCATATTATTTTTGGAGTTG
Nchet-6OR     ATCATGATGCTGCCCTATGGCGAGTGCCCATTGGTGATCAGCATATTATTTTTGGAGTTG

IB20          GTCGCCAAATCGCGAAAAGGACAGACTCGAAGGAGGATTCAGCGTTTCAGAACTTCATCG
Nchet-6OR     GTCGCCAAATCGCGAAAAGGACAGACTCGAAGGAGGATTCAGCGTTTCAGAACTTCATCG

IB20          CATACTACGAGGACTACGTGCGCCGGGACGATGATTGGAAAGATTATATGGCAGCTTACC
Nchet-6OR     CATACTACGAGGACTACGTGCGCCGGGACGATGATTGGAAAGATTATATGGCAGCTTACC

IB20          AAGCAGGAGAGGAGCAGGCCAAATTGAAGATGGGCAAGCACATGGACCGGGTTTTCTCAG
Nchet-6OR     AAGCAGGAGAGGAGCAGGCCAAATTGAAGATGGGCAAGCACATGGACCGGGTTTTCTCAG

IB20          AGGGATATTATATGGGCTTGCGGCATATGGAAGGAAAACGCCCGTACCTCACAGAGAATG
Nchet-6OR     AGGGATATTATATGGGCTTGCGGCATATGGAAGGAAAACGCCCGTACCTCACAGAGAATG

IB20          GATATCTAGGCATGGGTCCAGGGCTCTTACAGCCCGGCGACAAGGTGGTTGTATTTCACG
Nchet-6OR     GATATCTAGGCATGGGTCCAGGGCTCTTACAGCCCGGCGACAAGGTGGTTGTATTTCACG
```

```
IB20        GCGACGATATACCATATGTGGTACGACCGGTGCCCGGAAAGGGGGATAACACGTACCTTT
Nchet-6O    GCGACGATATACCATATGTGGTACGACCGGTGCCCGGAAAGGGGGATAACACGTACCTTT

IB20        TGATGGGGGAAGCATACTGCGATGGGATTATGGACGGGGAACTCGCTGATACGGCGGAGA
Nchet-6OR   TGATGGGGGAAGCATACTGCGATGGGATTATGGACGGGGAACTCGCTGATACGGCGGAGA

IB20        GGGAGGATTTCTATCTTGTCTGATGTGGTCTTTTCCTTTCAGTTTTTTTTTTCTTTCTCT
Nchet-6OR   GGGAGGATTTCTATCTTGTCTGATGTGGTCTTTTCCTTTCAGTTTTTTTTTTCTTTCTCT
                                 STOP
IB20        TTCTTTTTCTACAATTAGCTTCACGGTAGTGGCGGGCGTGTTGACCTTTTGGATATCGGC
Nchet-6OR   TTCTTTTTCTACAATTAGCTTCACGGTAGTGGCGGGCGTGTTGACCTTTTGGATATCGGC

IB20        GGATTGTGGGGGAAGTTGCAAGCTTGGGGCCTGGCCCACTCGCTCTTTTCTTCCACCAAA
Nchet-6OR   GGATTGTGGGGGAAGTTGCAAGCTTGGGGCCTGGCCCACTCGCTCTTTTCTTCCACCAAA

IB20        CCGCTGCAAGCCACCCCTTGGACACTCCATCGTGATTTCTTC----------------
Nchet-6OR   CCGCTGCAAGCCACCCCTTGGACACTCCATCGTGATTTCTTCACAACAAATATGCGTCAA
```

Appendix B

Sequence alignment of the pCOR1vd construct with wt *het-6*^{OR}, showing the replacement of the putative VIB-1 binding site (red box) with the *Bsi*WI restriction site (blue box). Alignment is from -250 to +4 of the wt *het-6*^{OR} ORF. The *het-6*^{OR} start codon is shown underlined in yellow

```
pCOR1vd     TGCTTGCCGT--------ACGACGCCATTTTACCTCGTCATGTAGGTAACCTCGCC
Nchet6-OR   TGCTTGCC-TAGCCAATCAC-ACGCCATTTTACCTCGTCATGTAGGTAACCTCGCC

pCOR1vd     ATGTAACCTCAACATGTGATCCTAGCGTCGATGGCCTCTTGGGTTCAGGTCAGGCA
Nchet6-OR   ATGTAACCTCAACATGTGATCCTAGCGTCGATGGCCTCTTGGGTTCAGGTCAGGCA

pCOR1vd     GCCATATTCGATGGATCTCCAGCCTCATCTCAAATTTCCAACATCATCGAGCTTGC
Nchet6-OR   GCCATATTCGATGGATCTCCAGCCTCATCTCAAATTTCCAACATCATCGAGCTTGC

pCOR1vd     AGCAGCCGCTTTTCTTGGAATTGTTGCCATTGATCCTACTTGCCTATCATTTGATG
Nchet6-OR   AGCAGCCGCTTTTCTTGGAATTGTTGCCATTGATCCTACTTGCCTATCATTTGATG

pCOR1vd     TCGTGCGCCGTCCGATCTCTTCGTCTTCATGG
Nchet6-OR   TCGTGCGCCGTCCGATCTCTTCGTCTTCATGG
                                    START
```

References

Aanen, D.K., Debets, A.J.M., Glass, N.L., and Saupe, S.J. (2010). Biology and genetics of vegetative incompatibility in fungi. In: Cellular and molecular biology of filamentous fungi. Eds Borkovich, K.A., and Ebbole, D.J. American Society for Microbiology. P 275-289. http://app.knovel.com/hotlink/toc/id:kpCMBFF00V/cellular-molecular-biology/cellular-molecular-biology

Anwar, M.M., Croft, J.H. and Dales R.B.G. (1993). Analysis of heterokaryon incompatibility between heterokaryon-compatibility (h-c) groups R and GL provides evidence that at least eight *het* loci control somatic incompatibility in *Aspergillus nidulans*. J. Gen. Microbiol. **139**, 1599-1603.

Araki, T., Nakao, H., Takeuchi, I. and Maeda, Y. (1994). Cell-cycle dependent sorting in the development of *Dictyostelium* cells. Dev. Biol. **162**, 221-228.

Barrangou, R., and Marraffini, L.A. (2014). CRISPR-Cas systems: Prokaryotes upgrade to adaptive immunity. Mol. Cell **54**, 234-244.

Bernstein, E., Caudy, A.A., Hammond, S.M., and Hannon, G.J. (2001). Role for a bidentate ribonuclease in the initiation step of RNA interference. Nature **18**(409), 363-366.

Balaburski, G.M., Hontz, R.D., and Murphy, M.E. (2010). p53 and ARF: unexpected players in autophagy. Trends in Cell Biology **20**(6), 363-369.

Balguerie, A., Dos Reis, S., Ritter, C., Chaignepain, S., Coulary-Salin, B., Forge, V., Bathany, L., Lascu, I., Schmitter, J.M., Riek, R. *et al*. (2003). Domain organization and structure-function relationship of the HET-s prion protein of *Podospora anserine*. EMBO J. **22**, 2071-2081.

Barrangou, R and Marraffini, L. A. (2014). CRISPR-Cas systems: prokaryotes upgrade to adaptive immunity. Mol. Cell **54**(2), 234-244.

Barreau, C., Iskandar, M., Loubradou, G., Levallois, V. and Begueret, J. (1998). The *mod-A* suppressor of nonallelic heterokaryon incompatibility in *Podospora anserina* encodes a proline-rich polypeptide involved in female organ formation. Genetics **149**, 915-926.

Bégueret, J., Turcq, B. and Clavé, C. (1994). Vegetative incompatibility in filamentous fungi: *het* genes begin to talk. Trends in Genetics **10**(12), 441-446.

Benichou, G. (1999). Direct and indirect antigen recognition: The pathways to allograft immune rejection. Frontiers in Bioscience **4**, 467-480.

Bischoff, J.R.., Friedman, P.N., Marshak, D.R., Prives, C., and Beach, B. (1990). Human p53 is phosphorylated by p60-cdc2 and cyclin B-cdc2. Proc. Natl. Acad. Sci. U.S.A. **87**, 4766-4770.

Boehm, T. (2006). Quality Control in Self/Nonself Discrimination. Cell **125**, 845–858.

Bork P, Holm L and Sander C. (1994). The immunoglobulin fold. Structural classification, sequence patterns and common core. J Mol Biol, **242**, 309–320.

Brady, C.A., and Attardi, L.D. (2010). p53 at a glance. J. Cell Sci. **123**, 2527-2532.

Brennan, C.A. and Anderson, K.V. (2004). *Drosophila*: The genetics of innate immune recognition and response. Ann. Rev. Immunol. **22**, 457-483.

Camamberi, E.B., Singer, M.J. and Selker, E.U. (1991). Recurrence of repeat-induced point mutation (RIP) in *Neurospora crassa*. *Genetics* **127**, 699-710.

Catalanotta, C., Azzalin, G., Macino, G., and Cogoni, C. (2002). Involvement of small RNAs and role of *qde* genes in the gene silencing pathway in *Neurospora*. Genes. Dev. **16**, 790-795.

Chevanne, D., Bastiaans, E., Debets, A., Saupe, S.J. Clavé, C., and Paoletti, M. (2009). Identification of the *het-r* vegetative incompatibility gene of *Podospora anserine* as a member of the fast-evolving HNWD gene family. Curr. Genet. **55**, 93-102.

Chevanne, D., Saupe, S.J., Clavé, C., Paoletti, M. (2010). WD-repeat instability and diversification of the *Podospora anserina hnwd* nonself recognition gene family. BMC Evol. Biol. **10**, 134.

Choi, G.H., Dawe, A.L. Churbanov, A, Smith, M.L., Milgroom, M.G. and Nuss, D.L. (2012). Molecular characterization of vegetative incompatibility genes that restrict hypovirus transmission in the Chestnut blight fungus *Cryphonectria parasitica*. Genetics **190**(1), 113-127.

Chu, S., DeRisi, J., Eisen, M., Mulholland, J., Botstein, D., and Brown, P.O. (1998). The transcriptional program of sporulation in budding yeast. Science **282**, 699-705.

Cogoni, C., Irelan, J.T., Schumacher, M., Schmidhauser, T.J., Selker, E.U. and Macino, G. (1996). Transgene silencing of the *al-1* gene in vegetative cells of *Neurospora* is mediated by a cytoplasmic effector and does not depend on DNA-DNA interactions

or DNA-methylation. *EMBO J.* **15**(12), 3153-3163.

Cogoni, C., and G. Macino**.** (1997). Isolation of quelling-defective (*qde*) mutants impaired in posttranscriptional transgene-induced gene silencing in *Neurospora crassa*. Proc. Natl. Acad. Sci. U.S.A. **94,** 10233-10238.

Cortesi, P., McCulloh, C.E., Song, H., Lin, H., and Milgroom, M.G. (2001). Genetic control of horizontal virus transmission in the Chestnut blight fungus, *Cryphonectria parasitica*. Genetics. **159**, 107-118.

Cortesi, P. and Milgroom, M.G. (1998). Genetics of vegetative incompatibility in *Cryphonectria parasitica*. Appl. Environ. Microbiol. **64**(8), 2988-2994.

Dang, Y., Yang, Q., Xue, Z., and Liu, Y. (2011). RNA interference in fungi: Pathways, functions and application. Eukar. Cell **10**(9), 1148-1155.

Davis, R.H., and de Serres, F.J. (1970). Genetic and microbiological research techniques for *Neurospora crassa*. Meth. Enzymol. **17**, 79-143.

Debets, A.J.M., and Griffiths, A.J.F. (1998). Polymorphism of *het*-genes prevents resource plundering in *Neurospora crassa*. Myco. Res. **102**(11), 1343-1349.

Debets, F., Yang, X., and Griffiths, A.J. (1994). Vegetative incompatibility in *Neurospora*: its effect on horizontal transfer of mitochondrial plasmids and senescence in natural populations. Curr. Genet. **26**(2), 113-119.

Dementhon, K., Iyer, G., and Glass, N.L. (2006). VIB-1 is required for expression of genes necessary for programmed cell death in *Neurospora crassa*. Eukaryot. Cell **5**(12), 2161-2173.

Derry, W.B., Putzke, A.P., and Rothman, J.H. (2001). *Caenorhabditis elegans* p53: Role in apoptosis, meiosis, and stress resistance. Science **294**(5542), 591-595.

Dodds, P.N. and Rothjen, J.P. (2010). Plant immunity: Towards an integrated view of plant-pathogen interactions. Nature Reviews **11**, 539-548.

Dos Reis, S., Coulary-Salin, B., Forge, V. Lascu, L, Bergueret, J and Suape, S.J. (2002). The HET-s prion protein of the filamentous fungus *Podospora anserina* aggregates *in Vitro* into amyloid-like fibrils. J. Biol. Chem. **277**(8), 8703-8706.

Doyle, C.E., Cheung, H.Y.K., Spence, K.L., and Saville, B.J. (2016). Unh1, an *Ustilago maydis* Ndt80-like protein, controls completion of tumor maturation, teliospore development, and meiosis. Fungal Genetics and Biology **94**, 54-68

Espagne, E., Balhadère, P., Bégueret, J., and Turcq, B. (1997). Reactivity in vegetative incompatibility of the HET-E protein of the fungus *Podospora anserina* is dependent on GTP-binding activity and a WD40 repeated domain. Mol. Gen. Genet. **256**, 620-627.

Farnebo, M., Bykov, V.J.N., and Wiman, K.G. (2010). The p53 tumor suppressor: A master regulator of diverse cellular processes and therapeutic target in cancer. Biochem. Biophys. Res. Comm. **396**(1), 85-89.

FGSC. 2008. Plasmid and Lambda Vectors. Accessed 10/06/2016. http://www.fgsc.net/plasmid/vector.html

Fiscella, M., Ulrich, S.J., Zambrano, N., Shields, M.T., Lin, D., Lees-Miller, S.O., Anderson, C.W., Mercer, W.E., and Appella, E. (1993). Mutation of the serine 15 phosphorylation site of human p53 reduces the ability of p53 to inhibit cell cycle progression. Oncogene **8**, 1519-1528.

Ghosh, A.K., and Varga, J. (2007). The transcriptional coactivator and acetyltransferase p300 in fibroblast biology and fibrosis. J. Cell. Physiol. **213**(3), 663-671.

Glass, N.L. and Dementhon, K. (2006). Nonself recognition and programmed cell death in filamentous fungi. Curr. Opin. Microbiol. **9**(6), 553-558.

Glass, N.L. and Kaneko, I. (2003). Fatal attraction: Nonself recognition and heterokaryon incompatibility in filamentous fungi. Eukaryot. Cell **2**(1), 1-8.

Glass, N.L., Grotelueschen, J., and Metzenberg, R.L. (1990). *Neurospora crassa* A mating type region. Proc. Natl. Acad. Sci. U.S.A. **87**, 4912-4916.

Glass, N.L., Jacobson, D.J. and Shiu, P.K.T. (2000). The genetics of hyphal fusion and vegetative incompatibility in filamentous ascomycete fungi. Annu. Rev. Genet. **34**, 165-186.

Grice, L.F. and Degnan, B.M. (2015). How to build an allorecognition system: A guide for prospective multicellular organisms. In 'Evolutionary Transitions to Multicellular Life'. Ruiz-Trillo, I. and Nedelcu, A.M. (Ed). (Netherlands: Springer) P 395-424.

Grissa, I., Vergnaud, G. and Pourcel, C. (2007). The CRISPRdb database and tools to display CRISPRs and to generate dictionaries of spacers and repeats. BMC Bioinfor. **8**, 172.

Gu, W., and Roeder, R.G. (1997). Activation of p53 sequence-specific DNA binding by

acetylation of the p53 C-terminal domain. Cell **90**(4), 595-606.

Gu, B., and Zhu, W-G. (2012). Surf the post-transcriptional modification network of p53 regulation. Int. J. Biol. Sci. **8**(5), 672-684.

Habu, T., Wakabayashi, N. Yoshida, K., Yomogida, K., Nishimune, Y., and Morita, T. (2004). p53 protein interacts specifically with the meiosis-specific mammalian RecA-like protein DMC1 in meiosis. Carcinogenesis **25**(6), 889-893.

Haupt, Y., Maya, R., Kazaz, A., and Oren, M. (1997). Mdm2 promotes the rapid degradation of p53. Nature **387**, 296-299.

Hirose, S, Benabentos, R, Ho, HI, and Kuspa, A. (2011). Self-recognition in social amoebae is mediated by allelic pairs of tiger genes. Science **333**, 467-470.

Hoebe, K., Janssen, E., and Beutler, B. (2004). The interface between innate and adaptive immunity. Nature Immunol. **5**, 971-974.

Honda, R., Tanaka, H., and Yasuda, H. (1997). Oncoprotein MDM2 is a ubiquitin ligase E3 for tumor suppressor p53. FEBS Lett. **420**, 25-27.

Horwich, A.L., and Weissman, J.S. (1997). Deadly conformations – Protein misfolding in prion diseases. Cell **89**, 499-510.

Hupp, T.R., Meek, D. W., Midgley, C.A., and Lane, D.P. (1992). Regulation of the specific DNA binding function of p53. Cell **71**, 875-886.

Hutchison, E.A. and Glass, N.L. (2012). Programmed cell death and heterokaryon incompatibility in filamentous fungi. In 'Biocommunication of Fungi'. Witzany, G., ed. (Netherlands: Springer), p 115-138.

Hutchison, E.A., and Glass, N.L. (2010). Interplay between NDT80 homologs and the protein kinase IME-2 regulates sexual development, but not meiosis, in *Neurospora crassa*. Genetics (Early online June 15, 2010); *DOI: 10.1534/genetics.110.117184*

Irelan, J.T. and Selker, E.U. (1996). Gene silencing in filamentous fungi: RIP, MIP and quelling. *J. Genet*. **75**(3), 313-324.

Ito, A., Lai, C-H., Zhao, X., Saito, S., Hamilton, M.H., Appella, E., and Yao, T-P. (2001). p300/CBP-mediated p53 acetylation is commonly induced by p53-activating agents and inhibited by MDM2. EMBO J. **20**(6), 1331-1340.

Iwasaki, A. and Medzhitov, R. (2010). Regulation of adaptive immunity by the innate immune system. Science **327**, 291-295.

Janeway, C.A., and Medzhitov, R. (2002). Innate immune recognition. Ann. Rev. Immunol. **20**, 197-216.

Jin, L., and Neiman, A.M. (2016). Post-transcriptional regulation in budding yeast meiosis. Curr. Genet. **62**, 313-315.

Jones, J.D.G. and Dangl, J.L. (2006). The plant immune system. Nature Reviews **444**, 323-329.

Kaneko, I., Dementhon, K., Xiang, Q., and Glass, N.L. (2006). Non-allelic interactions between *het-c* and a polymorphic locus, *pin-c*, are essential for nonself recognition and programmed cell death in *Neurospora crassa*. Genetics **172**, 1545-1555.

Katz, M.E., Braunberger, K., Yi, G., Cooper, S., Nonhebel, H.M., and Gondro, C. (2013). A p53-like transcription factor similar to Ndt80 controls the response to nutrient stress in the filamentous fungus, *Aspergillus nidulans*. [version 1; referees: 2 approved]. F1000Research **2**, 72.

Kim, H., Wright, S.J., Park, G., Ouyang, S., Kyrstofova, S., and Borkovich, K.A. (2012). Roles for receptors, pheromones, G proteins, and mating types during sexual reproduction in *Neurospora crassa*. Genetics **190**(4), 1389-1404.

King, N. (2004). The unicellular ancestry of animal development. Dev. Cell **7**, 313–325.

Kronstad, J.W. and Staben, C. (1997). Mating type in filamentous fungi. Annu. Rev. Genet. **31,** 245-276.

Kubbutat, M.H., Jones, S.N., and Vousden, K.H. (1997). Regulation of p53 stability by Mdm2. Nature **387**, 299-303.

Kurtz, J. (2003). Sex, parasites and resistance – an evolutionary approach. Zoology **106**, 327-339.

Lafontaine, D.L., and Smith, M.L. (2012). Diverse interactions mediate asymmetric incompatibility by the *het-6* supergene complex in *Neurospora crassa*. Fung. Genet. Biol. **49**, 65-73.

Lambris, J.D., Ricklin, D. and Geisbrecht, B.V. (2008). Complement evasion by human pathogens. Nature Reviews **6**, 132-142.

Lamoureux, J.S., and Glover, J.N.M. (2006). Principles of protein-DNA recognition revealed in the structural analysis of Ndt80-MSE DNA complexes. Structure **14**(3), 555-565.

Lamoureux, J.S., Stuart, D., Tsang, R., Wu, C., and Glover, J.N.M. (2002). Structure of the sporulation-specific transcription factor Ndt80 bound to DNA. EMBO J. **21**(21), 5587-5953.

Leach, C.K., Ashworth, J.M. and Garrod, D.R. (1973). Cell sorting out during the differentiation of mixtures of metabolically distinct populations of *Dictyostelium discoideum*. J. Embryol. Exp. Morph. **29**(3), 647-661.

Lee, H.C., Aalto, A.P., Yang, Q., Chang, S.S., Huang, G., Fisher, D., Cha, J., Poranen, M.M., Bamford, D.H., and Liu, Y. (2010). The DNA/RNA-dependent RNA polymerase QDE-1 generates aberrant RNA and dsRNA for RNAi in a process requiring replication protein A and a DNA helicase. PLoS Biol. **8**(10), e1000496.

Lee, J.T., and Gu, W. (2010). The multiple levels of regulation by p53 ubiquitination. Cell Death Differ. **17**(1), 86-92.

Lees-Miller, S.P., Chen Y-R., and Anderson, C.W. (1990) Human cells contain a DNA-activated protein kinase that phosphorylates simian virus 40 T antigen, mouse p53 and the human Ku autoantigen. Mol. Cell. Biol. **10**, 6472-6481.

Leslie, J.F. and Yamashiro, C.T. (1997). Effects of the *tol* mutation on allelic interactions at *het* loci in *Neurospora crassa*. Genome **40**, 834-840.

Maddocks, O.D.K., and Vousden, K.H. (2011). Metabolic regulation by p53. J. Mol. Med. **89**(3), 237-245.

Makeyev, E. V., and D. H. Bamford**.** (2002). Cellular RNA-dependent RNA polymerase involved in posttranscriptional gene silencing has two distinct activity modes. Mol. Cell **10,**1417-1427.

McGhee, K.E. (2006). The importance of life-history stage and individual variation in the allorecognition system of a marine sponge. *J. Exp. Mar. Biol. Ecol.* **333**(2), 241-250.Medzhitov, R. (2007). Recognition of microorganisms and activation of the immune response. Nature **449**(7164), 819+.

Medzhitov, R. (2007). Recognition of microorganisms and activation of the immune response. Nature **449**, 819-826.

Meek, D.W., Simon, S., Kikkawa, U., and Eckhart, W. (1990). The p53 tumor suppressor protein is phosphorylated at serine 389 by casein kinase II. EMBO J., **9**, 3253-3260.

Micali, C.O., and Smith, M.L. (2006). A nonself recognition gene complex in *Neurospora crassa*. Genetics **173**, 1991-2004.

Milne, D.M., Palmer, R.H., Campbell, D.G., and Meek, D.W. (1992). Phosphorylation of the hp53 tumor-suppressor protein at three N-terminal sites by a novel casein kinase I-like enzyme. Oncogene **7**, 1361-1369.

Mir-Rashed, N., Jacobson, D.J., Dehgany, M.R., Micali, O.C., and Smith, M.L. (2000). Molecular and functional analyses of incompatibility genes at *het-6* in a population of *Neurospora crassa*. Fung. Genet. Biol. **30**(3), 197-205.

Mojica, F.J.M., Díez-Villaseñor, C., García-Martínez, J., and Almendros, C. (2009). Short motif sequences determine the targets of the prokaryotic CRISPR defence system. Microbiology, **155**, 733-740.

Montano, S.P., Coté, M.L., Fingerman, I., Pierce, M., Vershon, A.K., and Georgiadis, M.M. (2002). Crystal structure of the DNA-binding domain from Ndt80, a transcriptional activator required for meiosis in yeast. PNAS **99**(22), 14041-14046.

Mourrain, P., C. Beclin, T. Elmayan, F. Feuerbach, C. Godon, J. B. Morel, D. Jouette, A. M. Lacombe, S. Nikic, N. Picault, K. Remoue, M. Sanial, T. A. Vo, and H. Vaucheret. (2000). *Arabidopsis SGS2* and *SGS3* genes are required for posttranscriptional gene silencing and natural virus resistance. Cell **101,**533-542.

Muthamilarasan, M. and Prasad, M. (2013). Plant innate immunity: An updated insight into defense mechanism. J. Biosci. **38**(2), 433-449.

Mylyk, O. M., 1975 Heterokaryon incompatibility genes in *Neurospora crassa* detected using duplication-producing chromosome rearrangements. Genetics **80,** 107–124.

Navarro-Sampedro, L., Olmedo, M., and Corrochano, L.M. (2007). How to transform *Neurospora crassa* by electroporation. http://fgsc.net/neurosporaprotocols/How%20to%20transform%20Nc%20by%20electroporation.pdf

Nikulenkov, F., Spinnler, C. Li, H., Tonelli, C., Shi, Y., Turunen, M., Kivioja, T. Ignatiev, I., Kel, A., Taipale, J., and Selivanova, G. (2012). Insights into p53 transcriptional function via genome-wide chromatin occupancy and gene expression analysis. Cell Death Differ. **19**(12), 1992-2002.

Oliner, J.D., Pietenpol, J.A., Thiagalingam, S., Gyuris, J., Kinzler, K.W., and Vogelstein, B. (1993). Oncoprotein MDM2 conceals the activation domain of tumor suppressor p53. Nature **362**, 857-860.

Paez-Espino, D., Morovic, W., Sun, C.L., Thomas, B.C., Ueda, K-I., Stahl, B., Barrangou, R., and Banfield, J.F. (2013). Strong bias in the bacterial CRISPR

elements that confer immunity to phage. Nature Comms. **4**, 1430.

Palm, N.W. and Medzhitov, R. (2009). Pattern recognition receptors and control of adaptive immunity. Immunol. Rev. **227**, 221-233.

Pandit, N.N. and Russo, V.E.A. (1992). Reversible inactivation of a foreign gene, *hph*, during the asexual cycle in *Neurospora crassa* transformants. *Mol. Gen. Genet*. **234**, 412-422.

Pant, V., and Lozano, G. (2014). Limiting the power of p53 through the ubiquitin proteasome pathway. Genes & Dev. **28**, 1739-1751.

Paoletti, M., Buck, K.W., and Brasier, C.M. (2006). Selective acquisition of novel mating type and vegetative incompatibility genes via interspecies transfer in the globally invading eukaryote *Ophiostoma novo-ulmi*. Mol. Ecol. **15**, 249-262.

Paoletti, M., and Clavé, C. (2007). The fungus-specific HET domain mediates programmed cell death in *Podospora anserine*. Eukaryot. Cell **6**(11), 2001-2008.

Philley, M.L., and Staben, C. (1994). Functional analyses of the *Neurospora crassa* MT a-1 mating type polypeptide. Genetics **137**, 715-722.

Reinhardt, H.C., and Schumacher, B. (2011). The p53 network: Cellular and systemic DNA damage responses in aging and cancer. Trends in Genetics **28**(3), 128-136.

Reshke, R. (2013). Developing a catalytically functional ribonucleotide reductase for *Neurospora crassa* that lacks heterokaryon incompatibility activity. MSc. Thesis. Carleton U. Retrieved from https://curve.carleton.ca/1934c019-dad7-4f1a-902a-6fe6068bd348

Rhounim, L., Rossignol, J-L. and Faugeron, G. (1992). Epimutation of repeated genes in *Ascobolus immersus*. *EMBO J.* **11**(12), 4451-4457.

Rokas, A. (2008). The origins of multicellularity and the early history of the genetic toolkit for animal development. Annu. Rev. Genet. **42**: 235-251.

Romano, N. and Macino, G. (1992). Quelling: transient inactivation of gene expression in *Neurospora crassa* by transformation with homologous sequences. *Mol. Microbiol.* **6**(22), 3343-3353.

Royer, J.C., and Yamashiro, C.T. (1992). Generation of transformable spheroplasts from mycelia macroconidia, microconidia and germinating ascospores of *Neurospora crassa*. Fungal Genet. Newsl. **39**, 76-79.

Sarkar, S., Iyer, G., Wu, J and Glass, N.L. (2002). Nonself recognition is mediated by HET-C heterocomplex formation during vegetative incompatibility. EMBO J. **21**(8), 4841-4850.

Saupe, S.J. (2000). Molecular genetics of heterokaryon incompatibility in filamentous ascomycetes. Microbiol. Mol. Biol. **64**(3), 489-502.

Saupe, S., Descamps, C., Turcq, B., and Bégueret, J. (1994). Inactivation of the *Podospora anserine* vegetative incompatibility locus *het-c*, whose product resembles a glycolipid transfer protein, drastically impairs ascospore production. Proc. Natl. Acad. Sci. U.S.A. **91**, 5927-5931.

Saupe, S.J., Kuldao, G.A, Smith, M.L., and Glass, N.L. (1996). The product of the *het-C* heterokaryon incompatibility gene of *Neurospora crassa* has characteristics of a glycine-rich cell wall protein. Genetics **143**, 1589-1600.

Scheidtmann, K.H., Mumby, M.C., Rundell, K., and Walter, G. (1991). Desphosphorylation of simian virus 40 large-T antigen and p53 protein by protein phosphatase 2A: inhibition by small-t antigen. Mol. Cell. Biol. **11**, 1996-2003.

SciStatCalc. 2013. Accessed 25 July, 2016. http://scistatcalc.blogspot.ca

Sheikh, M.S., and Fornace Jr. A.J. (2000). Role of p53 family members in apoptosis. J. Cell Phys. **182**, 171-181.

Shiu, P.K., and Glass, N.L. (1999). Molecular characterization of *tol*, a mediator of mating-type-associated vegetative incompatibility in *Neurospora crassa*. Genetics **151**(2), 545-555.

Siliciano, J.D., Canman, C.E., Taya, Y., Sakaguchi, K., Appella, E., and Kastan, M.B. (1997). DNA damage induces phosphorylation of the amino terminus of p53. Genes Dev. **11**, 3471-3481.

Smith M.L. and Lafontaine D.L. (2013). The fungal sense of nonself. In: Neurospora: Genomics and Molecular Biology. Eds. DP Kasbekar and K McCluskey, (Norfolk, UK: Horizon Scientific Press), p 9-19.

Smith, M.L., Micali, O.C., Hubbard, S.P., Mir-Rashed, N., Jacobson, D.J., and Glass, N.L. (2000). Vegetative incompatibility in the *het-6* region of *Neurospora crassa* is mediated by two linked genes. Genetics **155**, 1095-1104.

Smith, M.L., Yang, C.J., Metzenberg, R.L., and Glass, N.L. (1996). Escape from *het-6* incompatibility in *Neurospora crassa* partial diploids involves preferential deletion

within the ectopic segment. Genetics **144**, 523-531.

Smith, R.P., Wellman, K., Haidari, L., Masuda, H., and Smith, M.L. (2013). Nonself recognition through intermolecular disulfide bond formation of ribonucleotide reductase in *Neurospora*. Genetics **193**, 1175-1183.

Turcq, B., Denayrolles, M., and Begueret, J. (1990). Isolation of the two allelic incompatibility genes *s* and *S* of the fungus *Podospora anserine*. Curr. Genet. **17**(4), 297-303.

Vaillancourt, L.J., Raudaskoski, M., Specht, C.A. and Raper, C.A. (1997). Multiple genes encoding pheromones and a pheromone receptor define the Bβ1 mating-type specificity in *Schizophyllum commune*. Genetics **146**(2), 541-551.

Xiang, Q. and Glass, N.L. (2002). Identification of *vib-1*, a locus involved in vegetative incompatibility mediated by *het-c* in *Neurospora crassa*. Genetics **162**, 89-101.

Zhang, W., McClain, C., Gau, J-P., Guo, X-Y. D., and Deisseroth, A.B. (1994). Hyperphosphorylation of p53 induced by okadaic acid attenuates its transcriptional activation function. Canc. Res. **54**, 4448-4453.

Zhang, X-D., Qin, Z-H., and Wang, J. (2010). The role of p53 in cell metabolism. Act. Pharm. Sin. **31**, 1208-1212.